Highlighting Thermodynamic Coupling Effects in Alcohol/Water Pervaporation across Polymeric Membranes

Rajamani Krishna*

Van 't Hoff Institute for Molecular Sciences

University of Amsterdam

Science Park 904

1098 XH Amsterdam, The Netherlands

email: r.krishna@contact.uva.nl

Table of Contents

1 Preamble

The Supporting Information accompanying our article *Highlighting Thermodynamic Coupling Effects in Alcohol/Water Pervaporation across Polymeric Membranes* provides: (1) the F-H model parameters used in the phase equilibrium calculations, (2) detailed development of the M-S equations using volume fractions, and (3) input data on the M-S diffusivities.

All the calculations and simulations reported in this article were performed using MathCad 15.[1]

For ease of reading, this Supplementary material is written as a stand-alone document; as a consequence, there is some overlap of material with the main manuscript.

2 Flory-Huggins description of phase equilibrium

Polymer membranes are widely used for mixture separations; for an introduction to this topic see Wesselingh and Krishna.[2] The upstream compartment contains fluid mixtures that are either in the gaseous state at elevated pressures, or in the liquid state; see schematic in Figure S1.

2.1 The Flory-Huggins model for penetrants/polymer mixtures

The thermodynamics of sorption equilibrium of penetrants and polymer is most commonly described by the Flory-Huggins relations.[2-4] The Flory-Huggins equation in its simplest form deals with molecules that are similar chemically, but differ greatly in length. An example might be cross-linked polyethylene with the penetrant propane (C_3H_8). The Flory-Huggins model is based on the idea that the chain elements of the polymer arrange themselves randomly (but with the molecules remaining connected) on a three- dimensional lattice; see inset in Figure S1.

The Flory-Huggins model does not take effects of crystallization or other inhomogeneities into account. The resulting equation for the activity of the penetrant is a simple function of the volume fraction of the penetrant in the membrane. We use ϕ_i to denote the volume fraction of the penetrant species *i*; the volume fraction of species *i* is $\phi_i = c_i \overline{V_i}$ where c_i is the molar concentration, and $\overline{V_i}$ is the partial molar volume of the penetrant species *i*. Other concentration measures are listed in Table S1. The use of mole fractions is not convenient for description of the phase equilibrium of mixtures of penetrants in polymers, because the molar mass of the polymer chains are ill defined.[2]

The Flory-Huggins (F-H) model for binary mixture of penetrant (1) and polymer (indicated by subscript m) is

Flory-Huggins description of phase equilibrium

$$\ln a_1 = \ln(\phi_1) + (1-\phi_1) - \phi_m \frac{\overline{V_1}}{\overline{V_m}} + \chi_{1m}\phi_m^2 \qquad \phi_m = 1-\phi_1 \tag{S1}$$

Equation (S1) contains a non-ideality, or interaction parameter χ_{1m} that is assumed to be independent of the volume fraction. If $\chi_{1m} > 0$, the penetrant and polymer repel, or dislike, each other. If $\chi_{1m} < 0$, the penetrant and polymer attract each other. If $\chi_{1m} = 0$, the penetrant and polymer are similar in nature and there are no attractive or repulsive forces.

Figure S2 illustrates the influence of the interaction parameter χ_{1m} on the activity (a_1) and thermodynamic correction factor, $\Gamma = \frac{\partial \ln a_1}{\partial \ln \phi_1}$, that plays a pivotal role in diffusion (discussions on this are in the following sections). In these calculations, the ratio $\frac{\overline{V_1}}{\overline{V_m}} = 0$, i.e. the molar volume of the penetrant is negligible in comparison to the molar volume of the polymer. If χ_{1m} is positive, the solution can split into two phases for a range of volume fractions, one rich in polymer and one rich in solvent; the demixing zone is indicated in cyan in Figure S2.

If the interaction parameter χ_{1m} is dependent on the volume fractions, the F-H model for unary systems needs to be extended as follows

$$\ln a_1 = \ln(\phi_1) + (1-\phi_1) - (1-\phi_1)\frac{\overline{V_1}}{\overline{V_m}} + \chi_{1m}(1-\phi_1)^2 + \phi_1(1-\phi_1)^2 \frac{\partial \chi_{1m}}{\partial \phi_1} \tag{S2}$$

For ternary mixtures of two penetrants, 1 and 2, and the polymer (m), there are three interaction parameters in the F-H description of phase equilibrium: $\chi_{12}, \chi_{1m}, \chi_{2m}$. If each of the three interaction parameters $\chi_{12}, \chi_{1m}, \chi_{2m}$ are dependent on the volume fractions of the penetrants, ϕ_1, ϕ_2 the F-H model for the component activities a_1, a_2 of the penetrants in the polymer membrane (m) are

$$\begin{aligned}
\ln a_1 &= \ln(\phi_1) + (1-\phi_1) - \phi_2 \frac{\overline{V_1}}{\overline{V_2}} - \phi_m \frac{\overline{V_1}}{\overline{V_m}} + \left(\chi_{12}\phi_2 + \chi_{1m}\phi_m\right)\left(\phi_2 + \phi_m\right) - \chi_{2m}\frac{\overline{V_1}}{\overline{V_2}}\phi_2\phi_m - u_1u_2\phi_2\frac{\partial\chi_{12}}{\partial u_2} \\
&\quad - u_1u_2\phi_m\frac{\partial\chi_{1m}}{\partial u_2} - \phi_1\phi_m^2\frac{\partial\chi_{1m}}{\partial\phi_m} + \frac{\overline{V_1}}{\overline{V_2}}u_2^2\phi_m\frac{\partial\chi_{2m}}{\partial u_1} - \frac{\overline{V_1}}{\overline{V_2}}\phi_2\phi_m^2\frac{\partial\chi_{2m}}{\partial\phi_m} \\
\ln a_2 &= \ln(\phi_2) + (1-\phi_2) - \phi_1 \frac{\overline{V_2}}{\overline{V_1}} - \phi_m \frac{\overline{V_2}}{\overline{V_m}} + \left(\chi_{12}\phi_1\frac{\overline{V_2}}{\overline{V_1}} + \chi_{2m}\phi_m\right)\left(\phi_1 + \phi_m\right) - \chi_{1m}\frac{\overline{V_2}}{\overline{V_1}}\phi_1\phi_m + \frac{\overline{V_2}}{\overline{V_1}}u_1^2\phi_2\frac{\partial\chi_{12}}{\partial u_2} \\
&\quad + \frac{\overline{V_2}}{\overline{V_1}}u_1^2\phi_m\frac{\partial\chi_{1m}}{\partial u_2} - \frac{\overline{V_2}}{\overline{V_1}}\phi_1\phi_m^2\frac{\partial\chi_{1m}}{\partial\phi_m} - u_1u_2\phi_m\frac{\partial\chi_{2m}}{\partial u_1} - \phi_2\phi_m^2\frac{\partial\chi_{2m}}{\partial\phi_m}
\end{aligned} \tag{S3}$$

In eq (S3), we have defined $u_2 = \dfrac{\phi_2}{\phi_1+\phi_2}$; $\quad u_1 = 1-u_2 = \dfrac{\phi_1}{\phi_1+\phi_2}$; $\qquad \phi_m = 1-\left(\phi_1+\phi_2\right)$.

Equation (S3) corresponds precisely with equations (6) and (7) of Mulder et al.[5] The same set of extended equations are also given by Yang and Lue[6] and Varady et al.[7]

In the scenario in which the penetrant-membrane interaction parameters χ_{1m}, χ_{2m} are independent on the volume fractions of the penetrants, Equation (S3) simplifies to yield

$$\begin{aligned}
\ln a_1 &= \ln(\phi_1) + (1-\phi_1) - \phi_2 \frac{\overline{V_1}}{\overline{V_2}} - \phi_m \frac{\overline{V_1}}{\overline{V_m}} + \left(\chi_{12}\phi_2 + \chi_{1m}\phi_m\right)\left(\phi_2 + \phi_m\right) - \chi_{2m}\frac{\overline{V_1}}{\overline{V_2}}\phi_2\phi_m - u_1u_2\phi_2\frac{\partial\chi_{12}}{\partial u_2} \\
\ln a_2 &= \ln(\phi_2) + (1-\phi_2) - \phi_1 \frac{\overline{V_2}}{\overline{V_1}} - \phi_m \frac{\overline{V_2}}{\overline{V_m}} + \left(\chi_{12}\phi_1\frac{\overline{V_2}}{\overline{V_1}} + \chi_{2m}\phi_m\right)\left(\phi_1 + \phi_m\right) - \chi_{1m}\frac{\overline{V_2}}{\overline{V_1}}\phi_1\phi_m + \frac{\overline{V_2}}{\overline{V_1}}u_1^2\phi_2\frac{\partial\chi_{12}}{\partial u_2}
\end{aligned} \tag{S4}$$

2.2 The Flory-Huggins model for binary liquid mixtures

As a special (degenerate) case, eq (S3) can be applied to describe the component activities for binary *liquid phase* mixtures in the upstream compartment of the membrane. Let ϕ_1^L, ϕ_2^L represent the volume fractions of components 1 and 2 in the bulk liquid mixture. These volume fractions are related to the mass fractions ω_i^L in the bulk liquid mixture $\phi_i^L = \dfrac{\dfrac{\omega_i^L}{\rho_i^L}}{\displaystyle\sum_{i=1}^{n}\frac{\omega_i^L}{\rho_i^L}}$, where ρ_i^L is the liquid phase mass density of the penetrant species *i*. Other concentration measures, and inter-relations, are listed in Table S1. We also have the constraint $\phi_1^L + \phi_2^L = 1$. The component activities in the liquid mixture are obtained from

Equation (S3) by omitting terms containing χ_{1m} and χ_{2m}, and setting $\phi_m = 0$; $\phi_1^L + \phi_2^L = 1$, and $u_2^L = \frac{\phi_2^L}{\phi_1^L + \phi_2^L} = \phi_2^L$:

$$\ln a_1^L = \ln(\phi_1^L) + (1 - \frac{\overline{V_1}}{\overline{V_2}})\phi_2^L + \chi_{12}\left(\phi_2^L\right)^2 - \phi_1^L\left(\phi_2^L\right)^2 \frac{\partial \chi_{12}}{\partial \phi_2^L}$$
$$\ln a_2^L = \ln(\phi_2^L) + (1 - \frac{\overline{V_2}}{\overline{V_1}})\phi_1^L + \frac{\overline{V_2}}{\overline{V_1}}\chi_{12}\left(\phi_1^L\right)^2 + \frac{\overline{V_2}}{\overline{V_1}}\phi_2^L\left(\phi_1^L\right)^2 \frac{\partial \chi_{12}}{\partial \phi_2^L} \quad \text{(S5)}$$

Equation (S5) corresponds precisely with equations (9), and (10) of Mulder et al.[5] The χ_{12} is related to the excess Gibbs free energy

$$\chi_{12} = \frac{1}{x_1 \phi_2^L}\left[x_1 \ln(\frac{x_1}{\phi_1^L}) + x_2 \ln(\frac{x_2}{\phi_2^L}) + \frac{G^{excess}}{RT}\right]$$
$$\frac{G^{excess}}{RT} = x_1 \ln(\gamma_1) + x_2 \ln(\gamma_2) \quad \text{(S6)}$$

In Equation (S6), x_1, x_2 are liquid phase mole fractions $x_i = \frac{c_i}{c_t} = \frac{\frac{\omega_i^L}{M_i}}{\sum_{i=1}^{n}\frac{\omega_i^L}{M_i}} = \frac{\omega_i^L}{M_i}\overline{M}$, where M_i is the molar mass of component *i* (units kg mol^{-1}), and $\overline{M} = \sum_{i=1}^{n} x_i M_i$ is the mean molar mass of the mixture; see Table S1.

The interaction parameter χ_{12} for mixtures such as water/ethanol are strongly dependent on the liquid mixture composition. The excess Gibbs free energy $\frac{G^{excess}}{RT} = x_1 \ln(\gamma_1) + x_2 \ln(\gamma_2)$ can be calculated from activity coefficient models such as that of Wilson, NRTL, and UNIQUAC.[5, 6] Mulder et al.[5] have also shown that the dependence of χ_{12} on the volume fractions of components in the bulk liquid mixture can be expressed as a fourth-order polynomial in $u_2^L = \frac{\phi_2^L}{\phi_1^L + \phi_2^L} = \phi_2^L$

Flory-Huggins description of phase equilibrium

$$\chi_{12} = a + b\left(u_2^L\right) + c\left(u_2^L\right)^2 + d\left(u_2^L\right)^3 + e\left(u_2^L\right)^4; \quad \text{bulk liquid mixture}$$
$$u_2^L = \frac{\phi_2^L}{\phi_1^L + \phi_2^L} = \phi_2^L; u_1^L = \frac{\phi_1^L}{\phi_1^L + \phi_2^L} = \phi_1^L = 1 - u_2^L = 1 - \phi_2^L \quad \text{(S7)}$$

The use of the fourth-order polynomial expression is particularly convenient for the evaluation of the derivative $\frac{\partial \chi_{12}}{\partial \phi_2^L}$ in Equation (S5). The five coefficients, a, b, c, d, e can be determined by fitting of the Wilson, NRTL, and UNIQUAC models for $\frac{G^{excess}}{RT} = x_1 \ln(\gamma_1) + x_2 \ln(\gamma_2)$. For example, for ethanol/water mixtures, Hietaharju et al.[8] have determined temperature-dependent coefficients a, b, c, d, e by fitting the Wilson activity coefficient model parameters from the Aspen Plus simulation software databank (WILS-HOC, v8.8). In all the Flory-Huggins calculations presented in this article, the 4th order polynomial expressions are used to describe the volume fraction dependence of χ_{12}.

A significant contribution of Mulder et al.[5] is to demonstrate that the interaction parameter χ_{12} for the same two penetrants in the polymer membrane phase experiences the same composition dependence on the normalized volume fraction of component 2 within the membrane $u_2 = \frac{\phi_2}{\phi_1 + \phi_2}$, i.e.

$$\chi_{12} = a + b(u_2) + c(u_2)^2 + d(u_2)^3 + e(u_2)^4; \quad \text{polymer membrane phase}$$
$$u_2 = \frac{\phi_2}{\phi_1 + \phi_2}; u_1 = \frac{\phi_1}{\phi_1 + \phi_2} = 1 - u_2 \quad \text{(S8)}$$

2.3 List of Tables for Flory-Huggins description of phase equilibrium

Table S1. Concentration measures and inter-relationships.

Concentration measure	units	Inter-relation, constraint
x_i, mole fraction of species i	-	$x_i = \frac{c_i}{c_t} = \frac{\frac{\omega_i}{M_i}}{\sum_{i=1}^{n}\frac{\omega_i}{M_i}} = \frac{\omega_i}{M_i}\overline{M}; \sum_{i=1}^{n} x_i = 1$
ω_i, mole fraction of species i	-	$\omega_i = \frac{\rho_i}{\rho_t} = \frac{x_i M_i}{\sum_{i=1}^{n} x_i M_i} = \frac{x_i M_i}{\overline{M}}; \sum_{i=1}^{n} \omega_i = 1$
c_i, molar density of species i	mol m^{-3}	$c_i = \frac{\rho_i}{M_i}; \sum_{i=1}^{n} c_i = c_t = \text{mixture molar density} = \frac{1}{\overline{V}}$
ρ_i, mass density of species i	kg m^{-3}	$\rho_i = c_i M_i; \sum_{i=1}^{n} \rho_i = \rho_t = \text{mixture mass density}$
M_i, molar mass of species i	kg mol^{-1}	$\overline{M} = \sum_{i=1}^{n} x_i M_i = \text{mean molar mass of mixture}$
$\overline{V_i}$, partial molar volume of i	m^3 mol^{-1}	$\overline{V} = \sum_{i=1}^{n} x_i \overline{V_i} = \frac{1}{c_t} = \text{mean molar volume of mixture}$
ϕ_i, volume fraction of species i	-	$\phi_i = c_i \overline{V_i} = \frac{\frac{\omega_i}{\rho_i}}{\sum_{i=1}^{n}\frac{\omega_i}{\rho_i}}$

2.4 List of Figures for Flory-Huggins description of phase equilibrium

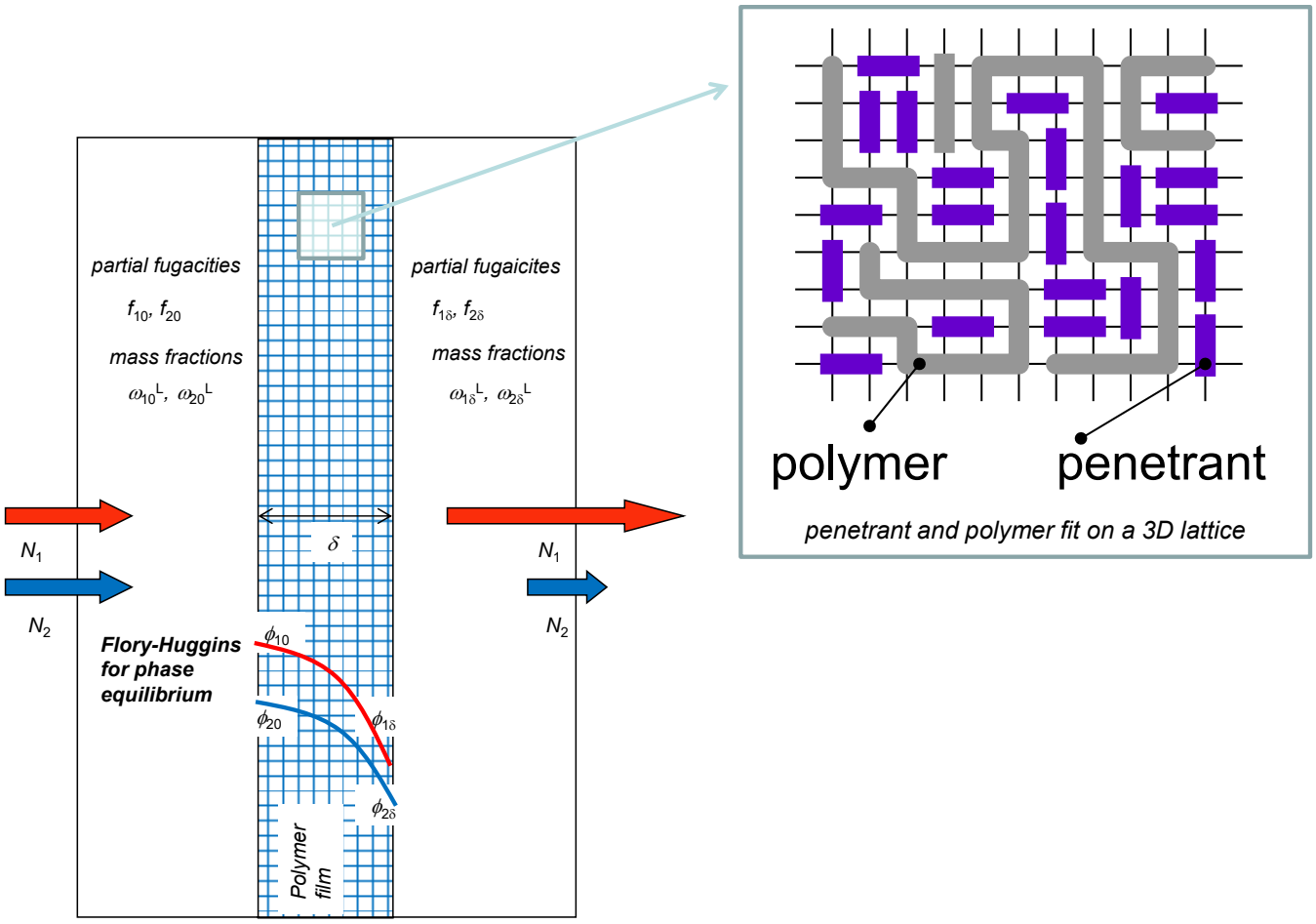

Figure S1. Schematic showing mixture permeation across polymeric membrane. The inset illustrates the Flory-Huggins lattice model.

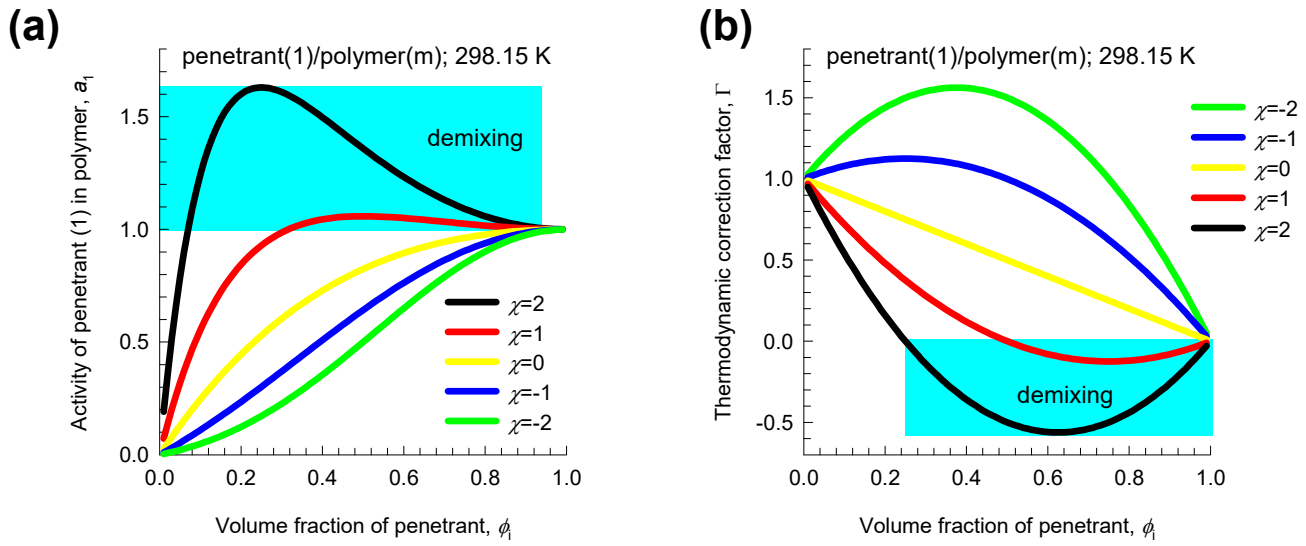

Figure S2. Influence of the interaction parameter on (a) the activity (a_1) and (b) thermodynamic correction factor, Γ. In these calculations, the ratio $\frac{\overline{V_1}}{V_m} = 0$, i.e. the molar volume of the penetrant is negligible in comparison to the molar volume of the polymer.

3 Maxwell-Stefan (M-S) diffusion formulation

3.1 The Maxwell-Stefan (M-S) description of diffusion in polymer solutions

We develop the Maxwell-Stefan (M-S) equations to describe the diffusion of *n* penetrants, 1, 2, 3,..*n* in a polymer matrix (m). The M-S equations represent a balance between the force exerted per mole of species *i* with the drag, or friction, experienced with each of the partner species in the mixture. We may expect that the frictional drag to be proportional to differences in the velocities of the diffusing species $(u_i - u_j)$, where u_i is the velocity of motion of the penetrant *i*. For diffusion in multicomponent polymer solutions such as acetone/cellulose acetate, $u_m \neq 0$, i.e. the polymer chains have a finite velocity of diffusion. For a mixture containing a total of *n* penetrants, 1, 2, 3,..*n* we write

$$
\begin{aligned}
-\frac{d\mu_1}{dz} &= \frac{RT}{Đ_{12}} X_2(u_1 - u_2) + \frac{RT}{Đ_{13}} X_3(u_1 - u_3) + \ldots + \frac{RT}{Đ_{1m}} X_m(u_1 - u_m) \\
-\frac{d\mu_2}{dz} &= \frac{RT}{Đ_{21}} X_1(u_2 - u_1) + \frac{RT}{Đ_{23}} X_3(u_2 - u_3) + \ldots + \frac{RT}{Đ_{2m}} X_m(u_2 - u_m) \\
&\cdots\cdots \\
-\frac{d\mu_n}{dz} &= \frac{RT}{Đ_{n1}} X_1(u_n - u_1) + \frac{RT}{Đ_{n2}} X_2(u_n - u_3) + \ldots + \frac{RT}{Đ_{nm}} X_m(u_n - u_m) \\
-\frac{d\mu_m}{dz} &= \frac{RT}{Đ_{m1}} X_1(u_m - u_1) + \frac{RT}{Đ_{m2}} X_2(u_m - u_3) + \ldots + \frac{RT}{Đ_{mn}} X_n(u_m - u_n)
\end{aligned}
\qquad \text{(S9)}
$$

The left members of equation (S9) are the negative of the gradients of the chemical potentials, with the units N mol^{-1}; it represents the driving force acting per mole of species 1, and 2. The subscript m refers to the polymer chain, that is regarded as the (*n*+1)*th* component in the mixture. The term $RT/Đ_{im}$ is interpreted as the drag or friction coefficient between the penetrant *i* and the polymer. The term $RT/Đ_{ij}$ is interpreted as the friction coefficient for the *i-j* pair of penetrants. The multiplier X_j in each of the right members represents a measure of the composition of component *j* in the mixture because we expect the friction to be dependent on the number of molecules of *j* relative to that of component *i*.

There are many possible choices for composition measures X_i. Written in terms of mole fractions, x_i, eqs (S9) are

$$
\begin{aligned}
-\frac{d\mu_1}{dz} &= \frac{RT}{Đ_{12}} x_2(u_1-u_2) + \frac{RT}{Đ_{13}} x_3(u_1-u_3) + \ldots + \frac{RT}{Đ_{1m}} x_m(u_1-u_m) \\
-\frac{d\mu_2}{dz} &= \frac{RT}{Đ_{21}} x_1(u_2-u_1) + \frac{RT}{Đ_{23}} x_3(u_2-u_3) + \ldots + \frac{RT}{Đ_{2m}} x_m(u_2-u_m) \\
&\cdots\cdots \\
-\frac{d\mu_n}{dz} &= \frac{RT}{Đ_{n1}} x_1(u_n-u_1) + \frac{RT}{Đ_{n2}} x_2(u_n-u_3) + \ldots + \frac{RT}{Đ_{nm}} x_m(u_n-u_m) \\
-\frac{d\mu_m}{dz} &= \frac{RT}{Đ_{m1}} x_1(u_m-u_1) + \frac{RT}{Đ_{m2}} x_2(u_m-u_3) + \ldots + \frac{RT}{Đ_{mn}} x_n(u_m-u_n)
\end{aligned}
\tag{S10}
$$

Only n of the chemical potential gradients $\frac{d\mu_i}{dz}$ are independent, because of the Gibbs-Duhem relationship

$$x_1 \frac{d\mu_1}{dz} + x_2 \frac{d\mu_2}{dz} + \cdots x_n \frac{d\mu_n}{dz} + x_m \frac{d\mu_m}{dz} = 0 \tag{S11}$$

The M-S formulation (S10) is consistent with the theory of irreversible thermodynamics. The Onsager Reciprocal Relations imply that the M-S pair diffusivities are symmetric

$$Đ_{ij} = Đ_{ji} \tag{S12}$$

3.2 Binary mixture permeation across polymer membranes

We apply the M-S formulation (S10) to describe permeation of two penetrants across a polymer membrane. We consider the polymer matrix to be stagnant, i.e. $u_m = 0$. For calculation of the chemical potential gradients, and activity gradients, using the Flory-Huggins model (i.e. eq (S3)) we need to reformulate the eq (S10) in terms of volume fractions instead of mole fractions.[7, 9, 10] Specifically for a binary mixture, we write

$$
\begin{aligned}
-\frac{1}{RT}\frac{d\mu_1}{dz} &= \frac{\phi_2(u_1-u_2)}{Đ_{12}^V} + \frac{\phi_m(u_1)}{Đ_{1m}^V} \\
-\frac{1}{RT}\frac{d\mu_2}{dz} &= \frac{\phi_1(u_2-u_1)}{Đ_{21}^V} + \frac{\phi_m(u_2)}{Đ_{2m}^V}
\end{aligned}
\tag{S13}
$$

Maxwell-Stefan (M-S) diffusion formulation

The modified M-S diffusivities $Đ_{12}^V$, $Đ_{21}^V$, $Đ_{1m}^V$, and $Đ_{2m}^V$ are related to the M-S diffusivities defined in terms of mole fractions, $Đ_{12}=Đ_{21}$, $Đ_{1m}$, $Đ_{2m}$ by $Đ_{12}^V = c_t Đ_{12}\overline{V_2} = \frac{Đ_{12}\overline{V_2}}{\overline{\overline{V}}}$, $Đ_{21}^V = c_t Đ_{21}\overline{V_1} = \frac{Đ_{21}\overline{V_1}}{\overline{\overline{V}}}$, $Đ_{1m}^V = c_t Đ_{1m}\overline{V_m} = \frac{Đ_{1m}\overline{V_m}}{\overline{\overline{V}}}$, and $Đ_{2m}^V = c_t Đ_{2m}\overline{V_m} = \frac{Đ_{2m}\overline{V_m}}{\overline{\overline{V}}}$. The symmetry constraint demanded by the Onsager Reciprocal Relations is

$$Đ_{12} = \frac{Đ_{12}^V}{\overline{\overline{V_2}}}\overline{V} = Đ_{21} = \frac{Đ_{21}^V}{\overline{\overline{V_1}}}\overline{V}; \quad \frac{Đ_{21}^V}{\overline{\overline{V_1}}} = \frac{Đ_{12}^V}{\overline{\overline{V_2}}} \tag{S14}$$

Commonly, the modified M-S diffusivities for penetrant-membrane interactions are taken to be functions of the volume fractions

$$Đ_{1m}^V = Đ_{1m}^V(0)\exp(\varepsilon_{11}\phi_1 + \varepsilon_{12}\phi_2); \quad Đ_{2m}^V = Đ_{2m}^V(0)\exp(\varepsilon_{21}\phi_1 + \varepsilon_{22}\phi_2) \tag{S15}$$

In eq (S15), the $\varepsilon_{11}, \varepsilon_{12}, \varepsilon_{21}, \varepsilon_{22}$ are termed plasticization coefficients.[8, 11]

In proceeding further, we re-write eqs (S13) by multiplying with ϕ_1, and ϕ_2, respectively,

$$\begin{aligned} -\frac{\phi_1}{RT}\frac{d\mu_1}{dz} &= \frac{\phi_1\phi_2(u_1-u_2)}{Đ_{12}^V} + \frac{\phi_1\phi_m(u_1)}{Đ_{1m}^V} \\ -\frac{\phi_2}{RT}\frac{d\mu_2}{dz} &= \frac{\phi_1\phi_2(u_2-u_1)}{Đ_{21}^V} + \frac{\phi_2\phi_m(u_2)}{Đ_{2m}^V} \end{aligned} \tag{S16}$$

Let us define the *volumetric* flux of component *i*, expressed as m^3 m^{-2} s^{-1} as $N_i^V = \phi_i u_i$. The molar flux of component *i*, expressed as mol m^{-2} s^{-1} is $N_i^{molar} = c_i u_i = \frac{\phi_i}{\overline{\overline{V_i}}}u_i = \frac{N_i^V}{\overline{\overline{V_i}}}$. The mass flux of component *i*, expressed as kg m^{-2} s^{-1} is $N_i^{mass} = \rho_i^L N_i^V = M_i N_i^{molar}$ where ρ_i^L is the liquid phase mass density of the pure component *i*. In terms of the volumetric fluxes of components,

In terms of the volumetric fluxes of components, $N_i^V = \phi_i u_i$, equation (S16) may be re-written as

Maxwell-Stefan (M-S) diffusion formulation

$$-\frac{\phi_1}{RT}\frac{d\mu_1}{dz}=\frac{\left(\phi_2 N_1^V-\phi_1 N_2^V\right)}{Đ_{12}^V}+\frac{\phi_m N_1^V}{Đ_{1m}^V}$$
$$-\frac{\phi_2}{RT}\frac{d\mu_2}{dz}=\frac{\left(\phi_1 N_2^V-\phi_2 N_1^V\right)}{Đ_{21}^V}+\frac{\phi_m N_2^V}{Đ_{2m}^V} \qquad \text{(S17)}$$

The first right members of eq (S17) quantify the contributions of 1-2 friction on the permeation fluxes.

The left members of eq (S17), containing the chemical potential gradients, may be expressed in terms of gradients in the volume fractions by introducing an 2×2 dimensional matrix of thermodynamic correction factors $[\Gamma]$:

$$\frac{\phi_i}{RT}\frac{d\mu_i}{dz}=\phi_i\frac{d\ln a_i}{dz}=\sum_{j=1}^{2}\Gamma_{ij}\frac{d\phi_j}{dz};\qquad \Gamma_{ij}=\frac{\phi_i}{\phi_j}\frac{\partial\ln a_i}{\partial\ln\phi_j};\quad i,j=1,2$$
$$\begin{bmatrix}\Gamma_{11} & \Gamma_{12}\\ \Gamma_{21} & \Gamma_{22}\end{bmatrix}=\begin{bmatrix}\phi_1\frac{\partial\ln a_1}{\partial\phi_1} & \phi_1\frac{\partial\ln a_1}{\partial\phi_2}\\ \phi_2\frac{\partial\ln a_2}{\partial\phi_1} & \phi_2\frac{\partial\ln a_2}{\partial\phi_2}\end{bmatrix} \qquad \text{(S18)}$$

The four elements $\Gamma_{11},\Gamma_{12},\Gamma_{21},\Gamma_{22}$ can be determined by analytic differentiation of eq (S3).

Furthermore, let us define a 2×2 dimensional matrix $[B]$ whose elements are given by

$$[B]=\begin{bmatrix}\frac{\phi_2}{Đ_{12}^V}+\frac{\phi_m}{Đ_{1m}^V} & -\frac{\phi_1}{Đ_{12}^V}\\ -\frac{\phi_2}{Đ_{21}^V} & \frac{\phi_1}{Đ_{21}^V}+\frac{\phi_m}{Đ_{2m}^V}\end{bmatrix}=\begin{bmatrix}B_{11} & B_{12}\\ B_{21} & B_{22}\end{bmatrix} \qquad \text{(S19)}$$

Combining eqs (S17), (S18), and (S19) we derive an explicit expression for the volumetric fluxes as functions of the gradients in the volume fractions:

$$(N^V)=-[B]^{-1}[\Gamma]\frac{d(\phi)}{dz};\quad \begin{pmatrix}N_1^V\\ N_2^V\end{pmatrix}=-\begin{bmatrix}B_{11} & B_{12}\\ B_{21} & B_{22}\end{bmatrix}^{-1}\begin{bmatrix}\phi_1\frac{\partial\ln a_1}{\partial\phi_1} & \phi_1\frac{\partial\ln a_1}{\partial\phi_2}\\ \phi_2\frac{\partial\ln a_2}{\partial\phi_1} & \phi_2\frac{\partial\ln a_2}{\partial\phi_2}\end{bmatrix}\begin{pmatrix}\frac{d\phi_1}{dz}\\ \frac{d\phi_2}{dz}\end{pmatrix} \qquad \text{(S20)}$$

Maxwell-Stefan (M-S) diffusion formulation

The matrix inversion $\begin{bmatrix} \Lambda_{11} & \Lambda_{12} \\ \Lambda_{21} & \Lambda_{22} \end{bmatrix} = \begin{bmatrix} B_{11} & B_{12} \\ B_{21} & B_{22} \end{bmatrix}^{-1}$ can be performed explicitly:

$$\begin{bmatrix} \Lambda_{11} & \Lambda_{12} \\ \Lambda_{21} & \Lambda_{22} \end{bmatrix} = \frac{\begin{bmatrix} \frac{\phi_1}{Đ_{21}^V} + \frac{\phi_m}{Đ_{2m}^V} & \frac{\phi_1}{Đ_{12}^V} \\ \frac{\phi_2}{Đ_{21}^V} & \frac{\phi_2}{Đ_{12}^V} + \frac{\phi_m}{Đ_{1m}^V} \end{bmatrix}}{\phi_m \left(\frac{\phi_1}{Đ_{21}^V Đ_{1m}^V} + \frac{\phi_2}{Đ_{12}^V Đ_{2m}^V} + \frac{\phi_m}{Đ_{1m}^V Đ_{2m}^V} \right)} = \frac{\begin{bmatrix} Đ_{1m}^V \left(\phi_m + \frac{\phi_1 Đ_{2m}^V}{Đ_{21}^V} \right) & Đ_{1m}^V \frac{\phi_1 Đ_{2m}^V}{Đ_{21}^V} \\ Đ_{2m}^V \frac{\phi_2 Đ_{1m}^V}{Đ_{12}^V} & Đ_{2m}^V \left(\phi_m + \frac{\phi_2 Đ_{1m}^V}{Đ_{12}^V} \right) \end{bmatrix}}{\phi_m \left(\frac{\phi_1 Đ_{2m}^V}{Đ_{21}^V} + \frac{\phi_2 Đ_{1m}^V}{Đ_{12}^V} + \phi_m \right)} \tag{S21}$$

The ratios $\frac{Đ_{1m}^V}{Đ_{12}^V}$, and $\frac{Đ_{2m}^V}{Đ_{21}^V}$ quantify the *degrees of correlations*; only one of these is independent because $\frac{Đ_{1m}^V}{Đ_{12}^V} = \frac{Đ_{2m}^V}{Đ_{21}^V} \frac{Đ_{1m}^V}{Đ_{2m}^V} \frac{\overline{V}_1}{\overline{\overline{V}}_2}$. Generally speaking for alcohol/water pervaporation processes, the thermodynamic coupling effects engendered by the off-diagonal elements of $\begin{bmatrix} \Gamma_{11} & \Gamma_{12} \\ \Gamma_{21} & \Gamma_{22} \end{bmatrix}$ are much stronger than the coupling effects caused by finite degrees of correlations: $\frac{Đ_{2m}^V}{Đ_{21}^V}$, $\frac{Đ_{1m}^V}{Đ_{12}^V}$.

The corresponding expression for the molar fluxes are

$$\begin{pmatrix} N_1^{molar} \\ N_2^{molar} \end{pmatrix} = -\begin{bmatrix} \frac{1}{\overline{\overline{V}}_1} & 0 \\ 0 & \frac{1}{\overline{\overline{V}}_2} \end{bmatrix} \begin{bmatrix} \Lambda_{11} & \Lambda_{12} \\ \Lambda_{21} & \Lambda_{22} \end{bmatrix} \begin{bmatrix} \phi_1 \frac{\partial \ln a_1}{\partial \phi_1} & \phi_1 \frac{\partial \ln a_1}{\partial \phi_2} \\ \phi_2 \frac{\partial \ln a_2}{\partial \phi_1} & \phi_2 \frac{\partial \ln a_2}{\partial \phi_2} \end{bmatrix} \begin{pmatrix} \frac{d\phi_1}{dz} \\ \frac{d\phi_2}{dz} \end{pmatrix} \tag{S22}$$

The corresponding expression for the mass fluxes are

$$\begin{pmatrix} N_1^{mass} \\ N_2^{mass} \end{pmatrix} = -\begin{bmatrix} \rho_1^L & 0 \\ 0 & \rho_2^L \end{bmatrix} \begin{bmatrix} \Lambda_{11} & \Lambda_{12} \\ \Lambda_{21} & \Lambda_{22} \end{bmatrix} \begin{bmatrix} \phi_1 \frac{\partial \ln a_1}{\partial \phi_1} & \phi_1 \frac{\partial \ln a_1}{\partial \phi_2} \\ \phi_2 \frac{\partial \ln a_2}{\partial \phi_1} & \phi_2 \frac{\partial \ln a_2}{\partial \phi_2} \end{bmatrix} \begin{pmatrix} \frac{d\phi_1}{dz} \\ \frac{d\phi_2}{dz} \end{pmatrix} \tag{S23}$$

3.3 Estimation 1-2 friction

We may estimate $Đ_{12}^{V}$ using the Vignes interpolation formula[12] for diffusion in binary liquid mixtures, adapted as follows[13]

$$\left(Đ_{12}^{V}/\overline{V_2}\right)=\left(Đ_{21}^{V}/\overline{V_1}\right)=\left(Đ_{1m}^{V}/\overline{V_2}\right)^{\phi_1/(\phi_1+\phi_2)}\left(Đ_{2m}^{V}/\overline{V_1}\right)^{\phi_2/(\phi_1+\phi_2)} \tag{S24}$$

with the limiting scenarios

$$\phi_2\to 0,\ Đ_{12}^{V}=Đ_{1m}^{V};\quad \phi_1\to 0,\ Đ_{21}^{V}=Đ_{2m}^{V} \tag{S25}$$

Alternatively, the degrees of correlations $\frac{Đ_{2m}^{V}}{Đ_{21}^{V}}$ may be fitted to match experimental data on mixture permeation.[14]

In the limiting scenario in which the degrees of correlations are considered to be of negligible importance, i.e. $\frac{Đ_{1m}^{V}}{Đ_{12}^{V}}\to 0;\quad \frac{Đ_{2m}^{V}}{Đ_{21}^{V}}\to 0$, the matrix $\begin{bmatrix}\Lambda_{11} & \Lambda_{12}\\ \Lambda_{21} & \Lambda_{22}\end{bmatrix}$ simplifies to yield

$$\begin{bmatrix}\Lambda_{11} & \Lambda_{12}\\ \Lambda_{21} & \Lambda_{22}\end{bmatrix}=\frac{1}{\phi_m}\begin{bmatrix}Đ_{1m}^{V} & 0\\ 0 & Đ_{2m}^{V}\end{bmatrix} \tag{S26}$$

Broadly speaking, we should expect the negligible 1-2 friction scenario to hold when the volume fractions of both penetrants in the membrane are negligibly small. Equation (S26) is used by Mulder et al.[15, 16] for modelling pervaporation of water (component 1), and ethanol (component 2) using cellulose acetate (polymer, component m) membrane.

3.4 Linearized model for binary mixture permeation across polymer membranes

In the linearized approach, we essentially assume that the volume fraction profiles for both penetrants across the membrane layer is linear. The elements of each of the two matrices $\begin{bmatrix}\Lambda_{11} & \Lambda_{12}\\ \Lambda_{21} & \Lambda_{22}\end{bmatrix}$, and $\begin{bmatrix}\Gamma_{11} & \Gamma_{12}\\ \Gamma_{21} & \Gamma_{22}\end{bmatrix}$ is evaluated by calculating the elements $Đ_{im}^{V}\left(\phi_{1,av},\phi_{2,av}\right)$, $Đ_{ij}^{V}\left(\phi_{1,av},\phi_{2,av}\right)$and $\Gamma_{ij}\left(\phi_{1,av},\phi_{2,av}\right)$ at

the arithmetic averaged volume fractions $\phi_{i,av} = \frac{(\phi_{i0} + \phi_{i\delta})}{2}$. With this assumption, the steady-state fluxes for permeation across a membrane of thickness δ are calculated explicitly using

$$\begin{pmatrix} N_1^V \\ N_2^V \end{pmatrix} = \frac{\begin{bmatrix} \Lambda_{11} & \Lambda_{12} \\ \Lambda_{21} & \Lambda_{22} \end{bmatrix}}{\delta} \begin{bmatrix} \Gamma_{11} & \Gamma_{12} \\ \Gamma_{21} & \Gamma_{22} \end{bmatrix} \begin{pmatrix} \phi_{10} - \phi_{1\delta} \\ \phi_{20} - \phi_{2\delta} \end{pmatrix}$$

$$\begin{pmatrix} N_1^{molar} \\ N_2^{molar} \end{pmatrix} = \begin{bmatrix} \frac{1}{\overline{\overline{V_1}}} & 0 \\ 0 & \frac{1}{\overline{\overline{V_2}}} \end{bmatrix} \begin{pmatrix} N_1^V \\ N_2^V \end{pmatrix} \qquad \text{(S27)}$$

$$\begin{pmatrix} N_1^{mass} \\ N_2^{mass} \end{pmatrix} = \begin{bmatrix} \rho_1^L & 0 \\ 0 & \rho_2^L \end{bmatrix} \begin{pmatrix} N_1^V \\ N_2^V \end{pmatrix}$$

The accuracy of the linearized model has been established in earlier work.[14] All the flux calculations reported in this article use the linearized eq (S27).

4 Modelling mixture permeation across polymeric membranes

4.1 Ethanol/water pervaporation across PDMS membrane

Polymeric membranes, such as polydimethylsiloxane (PDMS) membranes, have received considerable attention in the literature due to their hydrophobicity, and hence their capability to separate organics from dilute aqueous mixtures.[6, 8, 17, 18]

Below we present a re-analysis of the experimental data on pervaporation of ethanol/water mixtures reported by Hietaharju et al.[8] and Nasiri and Aroujalian,[18] with the objective of demonstrating the significant influence of thermodynamic coupling effects, embodied in the cross-coefficients of $\begin{bmatrix} \Gamma_{11} & \Gamma_{12} \\ \Gamma_{21} & \Gamma_{22} \end{bmatrix}$, on the pervaporation fluxes.

The first step is to establish the sorption equilibrium using the Flory-Huggins model. Figure S3 presents the experimental data of Yang and Lue[6] on the mass uptakes of penetrants ethanol (1) and water (2) in PDMS (m) at 298.15 K, plotted as function of the mass fraction of ethanol in the liquid feed mixture in the upstream compartment ω_1^L. The mass uptakes, expressed as kg penetrant per kg dry membrane, are related to the volume fractions ϕ_i in the membrane by

$$Uptake_i = \frac{\phi_i \rho_i^L}{\phi_m \rho_m}; \quad \phi_i = \frac{\dfrac{Uptake_i}{\rho_i^L}}{\dfrac{Uptake_1}{\rho_1^L} + \dfrac{Uptake_2}{\rho_2^L} + \dfrac{1}{\rho_m}} \tag{S28}$$

where $\rho_1^L, \rho_2^L, \rho_m$ are the densities of the liquid penetrants and membrane. The continuous solid lines are the Flory-Huggins calculations using the parameters reported by Hietaharju et al.;[8] see Table S2; The F-H calculations are in good agreement with the experimental data of Yang and Lue.[6]

Figure S4a presents calculations for the thermodynamic correction factors for the ternary mixture ethanol(1)/water(2)/PDMS(m) at 313 K, for varying mass fractions of ethanol (1) in the liquid feed

mixture in the upstream compartment ω_1^L. Particularly noteworthy are the negative values of the Γ_{12}. Figure S4b plots the ratios $\frac{\Gamma_{12}}{\Gamma_{11}}$, and $\frac{\Gamma_{21}}{\Gamma_{22}}$ as a function of the mass fraction of ethanol, ω_1^L, in the bulk liquid mixture in the upstream compartment. The large negative value of $\frac{\Gamma_{12}}{\Gamma_{11}}$ implies that the flux of ethanol is strongly influenced, i.e. suppressed, by the driving force for water transport. The value of $\frac{\Gamma_{21}}{\Gamma_{22}}$ is also negative, but smaller in magnitude than $\frac{\Gamma_{12}}{\Gamma_{11}}$.

Hietaharju et al.[8] report experimental data on the mass fluxes of the penetrants N_1^{mass}, N_2^{mass} for pervaporation of ethanol/water mixtures with varying mass fraction of ethanol, ω_1^L, in the bulk liquid mixture in the upstream compartment at temperatures T = 313 K, and 333 K. Hietaharju et al.[8] also report experimental data for vapor permeation in which the ethanol/water vapor mixture, in equilibrium with a ethanol/water liquid phase mixture at the corresponding dew point, is permeated across the PDMS membrane. For modelling their three sets of experiments, we use the linearized eq (S27), invoking the Vignes interpolation formula (S24). In the modelling procedure, eq (S15) is used to describe the penetrant-membrane interactions. For pervaporation across PDMS membranes, the volume fractions of water, ϕ_2, in the membrane are about one to two orders of magnitude lower than that of ethanol, ϕ_1, (cf. Figure S3), and therefore the plasticization coefficients $\varepsilon_{12}, \varepsilon_{22}$ are taken as zero. The fitted values of zero-occupancy M-S diffusivities, $Đ_{1m}^V(0), Đ_{2m}^V(0)$, and plasticization coefficients $\varepsilon_{11}, \varepsilon_{21}$ are specified in Table S3. It is noteworthy that we use the same set of plasticization coefficients for all three sets of experiments $\varepsilon_{11} = 5; \varepsilon_{12} = 0; \varepsilon_{21} = -18; \varepsilon_{22} = 0$. For further discussions on the interpretation and significance of negative values for ε_{21}, see Favre et al.[19] and Yang and Lue.[17]

Figure S5a,b compare the experimental mass fluxes with calculations using linearized eq (S27); the agreement is very good for all three sets. The permeation flux relations used by Hietaharju et al.[8] to model their own experiments do not account for thermodynamic coupling effects; see equations 28, and

29 of Hietaharju et al.[8] Consequently, the match of their model predictions with experiments are significantly poorer, especially for ethanol; see Figure 7 of their paper.

In order to highlight the importance of thermodynamic coupling, Figure S5c compares the mass fluxes of ethanol and water for pervaporation at 313 K, calculated using two different scenarios for $\begin{bmatrix}\Gamma_{11} & \Gamma_{12}\\ \Gamma_{21} & \Gamma_{22}\end{bmatrix}$. The continuous solid lines in Figure S5c represent model calculations using the linearized eq (S27), with proper evaluation of Γ_{ij} using the F-H eqs (S3). The dashed lines in Figure S5c represent model calculations using eq (S27) in which $\Gamma_{ij}=\delta_{ij}$, the Kronecker delta. In the scenario in which thermodynamic coupling effects are ignored, both the fluxes of ethanol and water are higher than for the scenario including thermodynamic coupling. The influence of thermodynamic coupling is essentially to reduce the permeation fluxes of both penetrants; this is akin to mutual-slowing down effects in zeolites,[20-22] engendered by molecular clustering phenomena due to hydrogen bonding between alcohol and water molecules. Figure S5d plots the ratios of the mass flux of ethanol to that of water as a function of the mass fraction of ethanol, ω_1^L, in the bulk liquid mixture in the upstream compartment. The influence of thermodynamic coupling is to suppress the flux of ethanol to a greater extent, leading to lower ethanol/water separation selectivity.

The analysis of the experimental data of Nasiri and Aroujalian[18] for pervaporation of ethanol(1)/water(2) mixtures across PDMS membrane, measured at three different temperatures T = 313 K, 323 K, and 333 K are presented in Figure S6. The fitted values of zero-occupancy M-S diffusivities, $Đ_{1m}^V(0), Đ_{2m}^V(0)$, and plasticization coefficients $\varepsilon_{11}, \varepsilon_{21}$ are specified in Table S4. It is noteworthy that we use the same set of plasticization coefficients for all three sets of experiments $\varepsilon_{11}=5; \varepsilon_{12}=0; \varepsilon_{21}=12; \varepsilon_{22}=0$. With these diffusivity data inputs, along with the F-H eqs (S3), the calculations using the linearized eq (S27) are shown by the continuous solid lines in Figure S6a,b; there is excellent agreement with the experimental data at all three temperatures.

Figure S6c compares the mass fluxes of ethanol and water for pervaporation at 313 K, calculated using two different scenarios for $\begin{bmatrix} \Gamma_{11} & \Gamma_{12} \\ \Gamma_{21} & \Gamma_{22} \end{bmatrix}$. The continuous solid lines in Figure S6c represent model calculations using the linearized eq (S27), with proper evaluation of Γ_{ij} using the F-H eqs (S3). The dashed lines in Figure S6c represent model calculations using eq (S27) in which $\Gamma_{ij} = \delta_{ij}$, the Kronecker delta. In the scenario in which thermodynamic coupling effects are ignored, both the fluxes of ethanol and water are higher than for the scenario including thermodynamic coupling. The influence of thermodynamic coupling is essentially to reduce the permeation fluxes of both penetrants; this is akin to mutual-slowing down effects in zeolites,[20-22] engendered by molecular clustering phenomena due hydrogen bonding between alcohol and water molecules. Figure S6d plots the ratios of the mass flux of ethanol to that of water as a function of the mass fraction of ethanol, ω_1^L, in the bulk liquid mixture in the upstream compartment. The influence of thermodynamic coupling is to suppress the flux of ethanol to a greater extent, leading to lower ethanol/water separation selectivity.

In eqs 19, and 20 of Nasiri and Aroujalian,[18] used to model their own experiments, the M-S diffusivities are modified in the following manner in order to explicitly account cluster formation leading to mutual slowing-down:

$$\begin{aligned} Đ_{1m}^V &= Đ_{1m}^V(0)\exp(\varepsilon_{11}\phi_1)\exp\left(-b_{11}\phi_1^2 - b_{12}\phi_1\phi_2\right); \\ Đ_{2m}^V &= Đ_{2m}^V(0)\exp(\varepsilon_{21}\phi_1)\exp\left(-b_{22}\phi_2^2 - b_{21}\phi_1\phi_2\right) \end{aligned} \tag{S29}$$

The set of plasticization, and clustering, coefficients, along with the zero-occupancy diffusivities are fitted for each of the three experiments sets; see Table 2 of their paper.

4.2 Water/ethanol pervaporation across cellulose acetate membrane

Cellulose acetate membranes are hydrophilic, and preferentially adsorb water from water/ethanol bulk liquid mixtures. The upstream face of the membrane is in equilibrium with water/ethanol liquid mixture of varying mass fractions. Figure S7a presents calculations of the volume fractions of penetrants water (1), ethanol (2) in a cellulose acetate (polymer, component m) at 293.15 K using the Flory-Huggins

parameters from Mulder et al.,[15, 16] the input data are specified in Table S5. The *x*-axis is the mass fraction of ethanol, ω_2^L, in the bulk liquid mixture in the upstream compartment.

Figure S7b presents calculations for the thermodynamic correction factors for the ternary mixture consisting of water (component 1), ethanol (component 2) and cellulose acetate (polymer, component m). Particularly noteworthy are the large negative values of the Γ_{12}. Figure S7c plots the ratios $\frac{\Gamma_{12}}{\Gamma_{11}}$, and $\frac{\Gamma_{21}}{\Gamma_{22}}$ as a function of the mass fraction of ethanol, ω_2^L, in the bulk liquid mixture in the upstream compartment. The large negative value of $\frac{\Gamma_{21}}{\Gamma_{22}}$ implies that the flux of ethanol is strongly influenced, i.e. suppressed, by the driving force for water transport. The value of $\frac{\Gamma_{12}}{\Gamma_{11}}$ is also negative, but smaller in magnitude than $\frac{\Gamma_{21}}{\Gamma_{22}}$.

In order to illustrate the influence of thermodynamic coupling on the pervaporation fluxes, we perform calculations using the input diffusivity data from Mulder et al;[15] see data in Table S5.

Following, Mulder et al.,[15] the modified M-S diffusivities for penetrant-membrane interactions are taken to be functions of the volume fractions

$$\begin{aligned} &Đ_{1m}^V = Đ_{1m}^V(0)\exp\left(\varepsilon_{11}\phi_1 + \varepsilon_{12}\phi_2\right); \quad Đ_{2m}^V = Đ_{2m}^V(0)\exp\left(\varepsilon_{21}\phi_1 + \varepsilon_{22}\phi_2\right); \\ &\varepsilon_{11} = \varepsilon_{12} = \varepsilon_{21} = \varepsilon_{22} = 7.3 \end{aligned} \tag{S30}$$

The molar fluxes are calculated using eq (S27), with the assumption that the volume fractions at the downstream face of the membrane are vanishingly small, $\phi_{1\delta} \approx 0; \phi_{2\delta} \approx 0$. The elements of each of the two matrices $\begin{bmatrix} \Lambda_{11} & \Lambda_{12} \\ \Lambda_{21} & \Lambda_{22} \end{bmatrix}$, and $\begin{bmatrix} \Gamma_{11} & \Gamma_{12} \\ \Gamma_{21} & \Gamma_{22} \end{bmatrix}$ is evaluated by calculating the elements $Đ_{im}^V\left(\phi_{1,av}, \phi_{2,av}\right)$, $Đ_{ij}^V\left(\phi_{1,av}, \phi_{2,av}\right)$and $\Gamma_{ij}\left(\phi_{1,av}, \phi_{2,av}\right)$ at the arithmetic averaged volume fractions $\phi_{i,av} = \frac{\left(\phi_{i0} + \phi_{i\delta}\right)}{2} \approx \frac{\phi_{i0}}{2}$. The Vignes interpolation formula (S24) is used for estimation of the degrees of correlation.

The continuous solid lines in Figure S8a are the calculations of the permeation fluxes using eq (S27) as function of the mass fraction of ethanol (2) in the liquid feed mixture in the upstream compartment, ω_2^L. The dashed lines in Figure S8a represent calculations of the permeation fluxes assuming a scenario in which the thermodynamic coupling effects are ignored and we assume which $\Gamma_{ij} = \delta_{ij}$, the Kronecker delta. The influence of thermodynamic coupling is that both water and ethanol fluxes are suppressed due to the transport of partners in the mixture.

In Figure S8b, the ratio of the molar flux of water to that of ethanol is plotted as function of the mass fraction of ethanol (2) in the liquid feed mixture in the upstream compartment, ω_2^L. Ignoring thermodynamic coupling leads to lower water/ethanol fluxes. The large negative value of $\frac{\Gamma_{21}}{\Gamma_{22}}$ implies that the flux of ethanol is more strongly influenced, i.e. suppressed, by the driving force for water transport.

For pervaporation of water/ethanol mixtures across the hydrophilic CA membrane, correlation effects are important, and serve to retard the transport of water, the more mobile partner in the mixture. In order to gauge the importance of correlation effects, Figure S8c compares the water/ethanol flux ratios for three additional scenarios for estimating the degrees of correlation, $\frac{Đ_{2m}^V}{Đ_{21}^V}$ besides the Vignes interpolation formula (S24): $\frac{Đ_{2m}^V}{Đ_{21}^V} = 0$, $\frac{Đ_{2m}^V}{Đ_{21}^V} = 5$, and $\frac{Đ_{2m}^V}{Đ_{21}^V} = 20$. Please note that the value $\frac{Đ_{1m}^V}{Đ_{12}^V}$ is calculable from $\frac{Đ_{1m}^V}{Đ_{12}^V} = \frac{Đ_{2m}^V}{Đ_{21}^V}\frac{Đ_{1m}^V}{Đ_{2m}^V}\frac{\overline{V_1}}{\overline{V_2}}$. The assertion $\frac{Đ_{2m}^V}{Đ_{21}^V} = 0$ essentially implies the use of eq (S31):

$$\begin{pmatrix} N_1^{molar} \\ N_2^{molar} \end{pmatrix} = -\begin{bmatrix} \frac{1}{\overline{V_1}} & 0 \\ 0 & \frac{1}{\overline{V_2}} \end{bmatrix} \frac{1}{(1-\phi_1-\phi_2)} \begin{bmatrix} Đ_{1m}^V & 0 \\ 0 & Đ_{2m}^V \end{bmatrix} \begin{bmatrix} \Gamma_{11} & \Gamma_{12} \\ \Gamma_{21} & \Gamma_{22} \end{bmatrix} \frac{\begin{pmatrix} \phi_{10}-\phi_{1\delta} \\ \phi_{20}-\phi_{2\delta} \end{pmatrix}}{\delta} \tag{S31}$$

With increasing degrees of correlation, the water/ethanol flux ratio decreases, as is to be expected.

4.3 Water/ethanol pervaporation across polyimide membrane

Figure S9a,b present calculations of the compositions of penetrants water (component 1), ethanol (component 2) in polyimide membrane (polymer, component m) at 293.15 K. The upstream face of the membrane is in equilibrium with water/ethanol liquid mixture of varying mass fractions. The Flory-Huggins model calculations are in good agreement with the experimental sorption data of Ni et al.,[23] as presented in Figures 1, and 2 of their paper. Water is preferentially sorbed in the polyimide membrane.

Figure S10a shows calculations of the elements of $[\Gamma]$ as function of the mass fraction of ethanol (2) in the liquid feed mixture in the upstream compartment, ω_2^L. The negative values of the off-diagonal elements Γ_{12}, Γ_{21} are particularly noteworthy. These negative values imply that the fluxes of both water and ethanol are negatively influenced by transport of the partners in the mixture.

Figure S10b plots the ratios of the elements of thermodynamic correction factors, $\frac{\Gamma_{12}}{\Gamma_{11}}, \frac{\Gamma_{21}}{\Gamma_{22}}$ as function of the mass fraction of ethanol (2) in the liquid feed mixture in the upstream compartment ω_2^L. The off-diagonal elements are significant fractions of the corresponding diagonal elements. Clearly, thermodynamic coupling should be expected to exert a significant influence on the permeation fluxes.

In order to underscore the significance of thermodynamic coupling we consider the experimental data of Ni et al.[23] on the volumetric fluxes of water, and ethanol, plotted in Figure S11a,b (indicated by symbols). For modeling purposes, the modified M-S diffusivities for penetrant-membrane interactions are taken to be functions of the volume fractions

$$\begin{aligned} &Đ_{1m}^V = Đ_{1m}^V(0)\exp\left(\varepsilon_{11}\phi_1 + \varepsilon_{12}\phi_2\right); \quad Đ_{2m}^V = Đ_{2m}^V(0)\exp\left(\varepsilon_{21}\phi_1 + \varepsilon_{22}\phi_2\right); \\ &\varepsilon_{11} = \varepsilon_{12} = \varepsilon_{21} = \varepsilon_{22} = 2 \end{aligned} \tag{S32}$$

The M-S diffusivities at zero volume fractions for penetrant-membrane interactions used in the calculations are the same as reported in Table 1 of Ni et al.[23]

$Đ_{1m}^V(0) = 25.5\times10^{-13}$ m^2 s^{-1}; $Đ_{2m}^V(0) = 2.1\times10^{-13}$ m^2 s^{-1}.

The continuous solid line in Figure S11a,b represent the estimates of the permeation fluxes using the linearized eq (S27). The best agreement with experiments is obtained the choice of the degree of correlaton $\frac{Đ^V_{2m}}{Đ^V_{21}} = 3; \quad Đ^V_{12} = Đ^V_{21}\frac{\overline{V_2}}{\overline{V_1}}$. Ni et al.[23] have also concluded that correlation effects cannot be ignored.

The dashed lines in Figure S11a,b represent calculations of the permeation fluxes assuming a scenario in which the thermodynamic coupling effects are ignored and we assume and $\Gamma_{ij} = \delta_{ij}$. The influence of thermodynamic coupling is that both water and ethanol fluxes are suppressed due to the transport of their partners in the mixture.

4.4 Water/ethanol pervaporation across PVA/PAN membrane

Figure S12a shows the experimental data (symbols) of Heintz and Stephan[24] for binary sorption of water/ethanol mixtures across a poly (vinyl alcohol) /poly (acrylonitrile) (PVA/PAN) composite membrane. The *x*-axis is the mass fraction of ethanol(2) in the liquid feed mixture in the upstream compartment ω_2^L. The continuous solid lines are the F-H model calculations using the input data in Table S7. There is very good agreement between the experimental sorption data and the F-H calculations.

Figure S12b presents calculations of the thermodynamic correction factors, Γ_{ij}, plotted as function of the mass fraction of ethanol(2) in the liquid feed mixture in the upstream compartment ω_2^L. The negative values of the off-diagonal elements Γ_{12}, Γ_{21} are particularly noteworthy. These negative values imply that the fluxes of both water and ethanol are negatively influenced by transport of the partners in the mixture. Figure S12c plots the ratios of the elements of thermodynamic correction factors, $\frac{\Gamma_{12}}{\Gamma_{11}}, \frac{\Gamma_{21}}{\Gamma_{22}}$ as function of the mass fraction of ethanol (2) in the liquid feed mixture in the upstream compartment ω_2^L. The large negative value of $\frac{\Gamma_{12}}{\Gamma_{11}}$ implies that the flux of water is strongly influenced, i.e.

suppressed, by the driving force for ethanol transport. The value of $\frac{\Gamma_{21}}{\Gamma_{22}}$ is also negative, but smaller in magnitude than $\frac{\Gamma_{12}}{\Gamma_{11}}$.

Figure S13a,b present calculations of the pervaporation fluxes for permeation of water(1)/ethanol(2) mixtures across PVA/PAN composite membrane (m) at 333 K. The continuous solid lines are flux calculations based on the linearized eq (S27); wherein the 1-2 friction is described by $\frac{Đ_{2m}^{V}}{Đ_{21}^{V}} = 4$, following previous work.[14] There is excellent agreement between the experimental data of Heintz and Stephan[25] (indicated by symbols) and the model calculations. The dashed lines are flux calculations in which thermodynamic correction factors are ignored, i.e. $\Gamma_{ij} = \delta_{ij}$. The influence of thermodynamic coupling is that both water and ethanol fluxes are suppressed due to the transport of their partners in the mixture.

4.5 CO_2/C_2H_6 permeation across XLPEO membrane

Figure S14a,b,c,d present calculations of the volume fractions of penetrants (a) CO_2 (1) and (b) C_2H_6 (2) in a cross-linked polyethylene oxide (XLPEO) membrane (m) at (a,b) 298.15 K, and (c, d) 263.15. The upstream face of the membrane is in equilibrium with CO_2/C_2H_6 mixtures of five different compositions. The F-H model calculations, indicated by the continuous solid lines, are in excellent agreement with the experimental data of Ribeiro and Freeman.[26] This is to be expected because the three interaction parameters $\chi_{12}, \chi_{1m}, \chi_{2m}$ were determined by fitting of the experimental data.

In order to highlight the importance of thermodynamic coupling effects, Figure S15a,b present the calculations of the four elements of the matrix of thermodynamic factors Γ_{ij}. In these calculations, the upstream face of the membrane is in equilibrium with 70% CO_2 gas mixture. Particularly noteworthy is the significant negative values of Γ_{12} for sorption at 263.15 K.

Figure S16a,b,c,d show the experimental data of Ribeiro et al.[27] for permeabilities of (a, c) CO_2 (1) and (b, d) C_2H_6 (2) for temperatures (a, b) 263.15 K, and (c, d) 293.15 K. The *x*-axis represents the partial fugacity of the permeants in the bulk gas phase in the upstream compartment. Five different mixture compositions are considered. We note that the permeability of C_2H_6 is strongly influenced (increased) by increasing proportion of CO_2 in the bulk gas phase mixture in the upstream compartment. On the other hand, the permeability of CO_2 is influenced to a much reduced extent by the feed mixture composition. The linearized solution to the M-S equation, eq (S27), wherein the 1-2 friction is described by $\frac{Đ_{2m}^{V}}{Đ_{21}^{V}} = 4$ following previous work,[14] are shown by the continuous solid lines. In this case thethermodynamic correction factors, Γ_{ij}, are calculated using the F-H eqs (S3). The M-S model captures, quantitatively, all the essential features of the composition dependence of the permeabilities of CO_2 and C_2H_6, for all feed mixture compositions at either temperature; see comparisons in

In order to highlight the importance of thermodynamic coupling on the permeation fluxes, Figure S17 presents parity plots of experimentally determined permeabilities with model predictions using two different scenarios for calculation of the thermodynamic correction factors, Γ_{ij}. In the first scenario (indicated by red circles), the Γ_{ij} are calculated using the F-H eqs (S3); in the second scenario (indicated by open squares), the thermodynamic coupling effects are ignored and $\Gamma_{ij} = \delta_{ij}$, the Kronecker delta. Ignoring thermodynamic coupling leads to overestimation of the permeabilities of both penetrants. In other words, thermodynamic coupling leads to mutual slowing down of the penetrants.

4.6 List of Tables for Modelling mixture permeation across polymeric membranes

Table S2. Flory-Huggins parameters for ethanol(1)/water(2)/PDMS(m).

The T-dependent coefficients a,b,c,d,e in the fourth-order polynomial expression $\chi_{12} = a + b(u_2) + c(u_2)^2 + d(u_2)^3 + e(u_2)^4$; $u_2 = \frac{\phi_2}{\phi_1 + \phi_2}\chi_{12}$ are provided in Table S2 of Hietaharju et al.[8] The penetrant-membrane parameters χ_{1m}, χ_{2m} are described using the model of Yang and Lue:[6] $\chi_{1m} = a_{1m}(T) + \frac{b_{1m}(T)}{(1 + c_{1m}(T)\phi_m)^2}$; $\chi_{2m} = a_{2m}(T) + \frac{b_{2m}(T)}{(1 + c_{2m}(T)\phi_m)^2}$. The T-dependent coefficients are provided in Table 1 of Hietaharju et al.[8]

The mass densities and molar volumes used in the F-H calculations are

$\overline{V_1} = 58.69 \times 10^{-6}$ m^3 mol^{-1}; $\overline{V_2} = 18 \times 10^{-6}$ m^3 mol^{-1}

$\frac{\overline{V_1}}{V_m} \approx 0; \frac{\overline{V_2}}{V_m} \approx 0; \rho_{1L} = 785; \rho_{2L} = 997; \rho_m = 965$ kg m^{-3}

Membrane thickness: $\delta = 1.3 \times 10^{-7}$ m.

Table S3. Diffusivity data for modelling of Hietaharju experiments for ethanol(1)/water(2)/PDMS(m).

Hietaharju et al.[8] report three sets of experimental data for pervaporation of ethanol(1)/water(2) mixtures across PDMS membrane of thickness $\delta = 80\times10^{-6}$ m.

The inputs used for the Maxwell-Stefan diffusivities and plasticization coefficients

$Đ_{1m}^{V} = Đ_{1m}^{V}(0)\exp(\varepsilon_{11}\phi_1 + \varepsilon_{12}\phi_2)$; $Đ_{2m}^{V} = Đ_{2m}^{V}(0)\exp(\varepsilon_{21}\phi_1 + \varepsilon_{22}\phi_2)$ for the three sets are as follows.

Set I: Pervaporation with liquid ethanol(1)/water(2) mixture in upstream compartment at T = 313 K

$Đ_{1m}^{V}(0) = 1.3\times10^{-10}$ m^2 s^{-1}; $Đ_{2m}^{V}(0) = 2.0\times10^{-10}$ m^2 s^{-1}

Set II: Pervaporation with liquid ethanol(1)/water(2) mixture in upstream compartment at T = 333 K

$Đ_{1m}^{V}(0) = 0.75\times10^{-10}$ m^2 s^{-1}; $Đ_{2m}^{V}(0) = 3.8\times10^{-10}$ m^2 s^{-1}

Set III: Vapor phase permeation of ethanol(1)/water(2) mixture

$Đ_{1m}^{V}(0) = 3\times10^{-11}$ m^2 s^{-1}; $Đ_{2m}^{V}(0) = 12\times10^{-10}$ m^2 s^{-1}

For all three sets of experiments the same set of plasticization coefficients were used:

$\varepsilon_{11} = 5; \varepsilon_{12} = 0; \varepsilon_{21} = -18; \varepsilon_{22} = 0$

Table S4. Diffusivity data for modelling of Nasiri experiments for ethanol(1)/water(2)/PDMS(m).

Nasiri and Aroujalian[18] report three sets of experimental data for pervaporation of ethanol(1)/water(2) mixtures across PDMS membrane of thickness $\delta = 40\times10^{-6}$ m. The inputs used for the Maxwell-Stefan diffusivities and plasticization coefficients

$Đ_{1m}^{V} = Đ_{1m}^{V}(0)\exp(\varepsilon_{11}\phi_1 + \varepsilon_{12}\phi_2)$; $Đ_{2m}^{V} = Đ_{2m}^{V}(0)\exp(\varepsilon_{21}\phi_1 + \varepsilon_{22}\phi_2)$ for the three sets are as follows.

Set I: Pervaporation with liquid ethanol(1)/water(2) mixture in upstream compartment at T = 313 K

$Đ_{1m}^{V}(0) = 1.0\times10^{-9}$ m^2 s^{-1}; $Đ_{2m}^{V}(0) = 1.9\times10^{-9}$ m^2 s^{-1}

Set II: Pervaporation with liquid ethanol(1)/water(2) mixture in upstream compartment at T = 323 K

$Đ_{1m}^{V}(0) = 0.75\times10^{-9}$ m^2 s^{-1}; $Đ_{2m}^{V}(0) = 2.5\times10^{-9}$ m^2 s^{-1}

Set III: Pervaporation with liquid ethanol(1)/water(2) mixture in upstream compartment at T = 323 K

$Đ_{1m}^{V}(0) = 0.65\times10^{-9}$ m^2 s^{-1}; $Đ_{2m}^{V}(0) = 3.3\times10^{-9}$ m^2 s^{-1}

For all three sets of experiments the same set of plasticization coefficients were used:

$\varepsilon_{11} = 5; \varepsilon_{12} = 0; \varepsilon_{21} = 12; \varepsilon_{22} = 0$

Table S5. Thermodynamics and diffusion data for water/ethanol/cellulose acetate.

The Flory-Huggins parameters for penetrants water (component 1) and ethanol (Component 2) in cellulose acetate (CA) membrane (indicated by subscript m) at T = 293.15 K. The data are taken from Mulder et al.:[5, 15, 16]

$$\chi_{12} = a + b(u_2) + c(u_2)^2 + d(u_2)^3 + e(u_2)^4; \quad u_2 = \frac{\phi_2}{\phi_1 + \phi_2}$$

$$a = 0.9820; b = -1.3483; c = 4.15; d = -3.3116; e = 0.8897;$$

$$\chi_{1m} = 1.4; \chi_{2m} = 1.1;$$

$$\overline{V_1} = 18 \times 10^{-6} \text{ m}^3 \text{ mol}^{-1}$$

$$\frac{\overline{V_1}}{\overline{V_2}} = 0.309; \frac{\overline{V_1}}{\overline{V_m}} = 0.002; \frac{\overline{V_2}}{\overline{V_m}} = 0.00647;$$

Modified Maxwell-Stefan diffusivities for permeation of penetrants water (component 1) and ethanol (Component 2) across a cellulose acetate (CA) membrane (indicated by subscript m) at T = 293.15 K. The data are taken from the legend to Figure 5 of Mulder and Smolders.[15]

$$Đ_{1m}^{V}(0) = 8.8 \times 10^{-12} \text{ m}^2 \text{ s}^{-1}$$

$$Đ_{2m}^{V} = 6 \times 10^{-12} \text{ m}^2 \text{ s}^{-1}$$

$$\delta = 20 \times 10^{-6} \quad \text{m}$$

$$\varepsilon_{11} = \varepsilon_{12} = \varepsilon_{21} = \varepsilon_{22} = 7.3$$

Table S6. Thermodynamics and diffusion data for water/ethanol/polyimide.

The Flory-Huggins parameters for penetrants water (1) and ethanol (2) in Polyimide membrane (indicated by subscript m) at T = 293.15 K. The data are based on the information provided from Ni et al.[23] The χ_{12} parameters are taken to be the same as for water/ethanol/CA.

$$\chi_{12} = a + b(u_2) + c(u_2)^2 + d(u_2)^3 + e(u_2)^4; \quad u_2 = \frac{\phi_2}{\phi_1 + \phi_2}$$

$$a = 0.9820; b = -1.3483; c = 4.15; d = -3.3116; e = 0.8897;$$

$$\chi_{1m} = 1.4; \chi_{2m} = 2.2 + 0.7\left(\frac{\phi_1}{\phi_1 + \phi_2}\right);$$

$$\overline{V_1} = 18 \times 10^{-6} \text{ m}^3 \text{ mol}^{-1}$$

$$\frac{\overline{V_1}}{\overline{V_2}} = 0.309; \frac{\overline{V_1}}{V_m} \approx 0.002; \frac{\overline{V_2}}{V_m} = 0.00649;$$

Membrane thickness: $\delta = 20 \times 10^{-6}$ m .

Modified Maxwell-Stefan diffusivities for permeation of penetrants water (component 1) and ethanol (Component 2) across the polyimide membrane (indicated by subscript m) at T = 293.15 K. The data on modified M-S diffusivities at zero volume fractions are taken from Table 1 of Ni et al.[23]. The exponential model is used to describe the variation of the modified M-S diffusivities on the volume fractions $Đ_{1m}^{V}(0) = 25.5 \times 10^{-13}$ m^2 s^{-1} $Đ_{2m}^{V}(0) = 1.5 \times 10^{-13}$ m^2 s^{-1} . The 1-2 friction is described by $\frac{Đ_{2m}^{V}}{Đ_{21}^{V}} = 3$.

$$\varepsilon_{11} = \varepsilon_{12} = \varepsilon_{21} = \varepsilon_{22} = 5$$

Table S7. Thermodynamics and diffusion data for water/ethanol/PVA/PAN.

Flory-Huggins parameters for permeation of penetrants water (1) and ethanol (2) across a poly (vinyl alcohol) /poly (acrylonitrile) (PVA/PAN) composite membrane (indicated by subscript m) at T = 333 K. The χ_{12} parameters were taken to be the same as for water/ethanol/CA. The values of χ_{1m}, χ_{2m} were chosen to match the experimental sorption data presented in Figure 2 of Heintz and Stephan.[24]

$$\chi_{12} = a + b(u_2) + c(u_2)^2 + d(u_2)^3 + e(u_2)^4; \quad u_2 = \frac{\phi_2}{\phi_1 + \phi_2}$$

$$a = 0.9820; b = -1.3483; c = 4.15; d = -3.3116; e = 0.8897;$$

$$\chi_{1m} = 0.65; \chi_{2m} = 1.75$$

$$\overline{V_1} = 18 \times 10^{-6} \text{ m}^3 \text{ mol}^{-1}; \overline{V_2} = 58.4 \times 10^{-6} \text{ m}^3 \text{ mol}^{-1}$$

$$\frac{\overline{V_1}}{V_m} \approx 0; \frac{\overline{V_2}}{V_m} \approx 0; \rho_{1L} = 1000; \rho_{2L} = 789; \rho_m = 1200 \quad \text{kg m}^{-3}$$

Membrane thickness: $\delta = 1.3 \times 10^{-7}$ m.

Modified Maxwell-Stefan diffusivities for permeation of penetrants water (1) and ethanol (2) across the PVA/PAN (indicated by subscript m) at T = 333 K. The M-S diffusivities for water and ethanol penetrants are assumed to follow an exponential dependence on the volume fractions

$Đ_{1m}^{V}(0) = 7.5 \times 10^{-14}$ m^2 s^{-1}

$Đ_{2m}^{V}(0) = 0.35 \times 10^{-14}$ m^2 s^{-1}. The 1-2 friction is quantified by $\frac{Đ_{2m}^{V}}{Đ_{21}^{V}} = 3$.

$\varepsilon_{11} = \varepsilon_{12} = \varepsilon_{21} = \varepsilon_{22} = 2$

Table S8. Thermodynamics and diffusion data for CO_2/C_2H_6/XLPEO at 263.15 K.

Flory-Huggins parameters for permeation of penetrants CO_2 (1) and C_2H_6 (2) across a cross-linked polyethylene oxide (XLPEO) membrane (indicated by subscript m) at T = 263.15 K. The input parameters are based on calculations using the information presented in Appendix A of Ribeiro et al.[9] In the Supplementary material of the paper by Krishna,[13] detailed comparison of experimental phase equilibrium data with predictions of the F-H equations are provided.

$f_{1,sat} = 21\times10^5$ Pa; $f_{2,sat} = 14.5\times10^5$ Pa

$\chi_{12} = -28.2 - \frac{44.3}{\ln(\phi_1)}$; $\chi_{1m} = 1.0421 + 12.3\phi_2$; $\chi_{2m} = 2.421 + 4.76\sqrt{\phi_1}$

$\overline{V_1} = 3.31\times10^{-5}$ m^3 mol^{-1}; $\overline{V_2} = 4.14\times10^{-5}$ m^3 mol^{-1}

Modified Maxwell-Stefan diffusivities for permeation of penetrants CO_2 (component 1) and C_2H_6 (Component 2) across a cross-linked polyethylene oxide (XLPEO) membrane (indicated by subscript m) at T = 263.15 K.

Input data for diffusivities used in the mixture permeability calculations:

$Đ_{1m}^V = 100\times10^{-12}\exp(8(\phi_1+\phi_2))$ m^2 s^{-1}
$Đ_{2m}^V = 38\times10^{-12}\exp(9(\phi_1+\phi_2))$ m^2 s^{-1}. The magnitude of 1-2 friction is described by $\frac{Đ_{2m}^V}{Đ_{21}^V} = 4$, following previous work.[14]

Table S9. Thermodynamics and diffusion data for CO_2/C_2H_6/XLPEO at 298.15 K.

Flory-Huggins parameters for permeation of penetrants CO_2 (1) and C_2H_6 (2) across a cross-linked polyethylene oxide (XLPEO) membrane (indicated by subscript m) at T = 298.15 K. The input parameters are based on calculations using the information presented in Appendix A of Ribeiro et al.[9] In the Supplementary material of the paper by Krishna,[13] detailed comparison of experimental phase equilibrium data with predictions of the F-H equations are provided.

$f_{1,sat} = 43\times10^5$ Pa; $f_{2,sat} = 28\times10^5$ Pa

$\chi_{12} = 1.52$; $\chi_{1m} = 0.9085$; $\chi_{2m} = 2.0804$

$\overline{V_1} = 4.174\times10^{-5}$ m^3 mol^{-1}; $\overline{V_2} = 6.04\times10^{-5}$ m^3 mol^{-1}

Modified Maxwell-Stefan diffusivities for permeation of penetrants CO_2 (component 1) and C_2H_6 (Component 2) across a cross-linked polyethylene oxide (XLPEO) membrane (indicated by subscript m) at T = 298.15 K.

Input data for diffusivities used in the mixture permeability calculations:

$Đ_{1m}^V = 100\times10^{-12}\exp(8(\phi_1+\phi_2))$ m^2 s^{-1}

$Đ_{2m}^V = 38\times10^{-12}\exp(9(\phi_1+\phi_2))$ m^2 s^{-1}. The magnitude of 1-2 friction is described by $\frac{Đ_{2m}^V}{Đ_{21}^V} = 4$, following previous work.[14]

4.7 List of Figures for Modelling mixture permeation across polymeric membranes

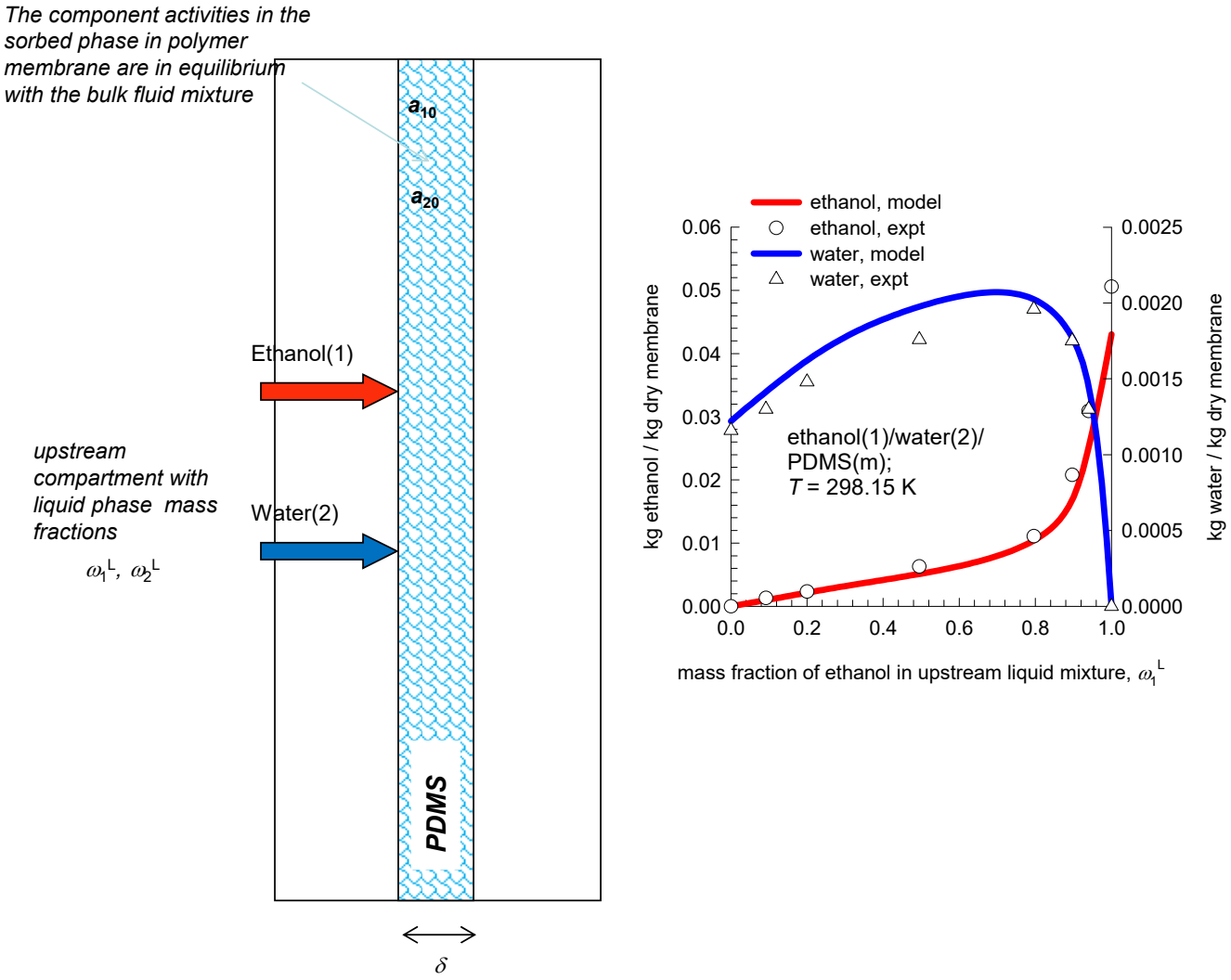

Figure S3. Experimental data (indicated by symbols) of Yang and Lue[6] of the mass uptakes of penetrants ethanol (1) and water (2) in PDMS (m) at 298.15 K, plotted as function of the mass fraction of ethanol in the liquid feed mixture in the upstream compartment ω_1^L. The continuous solid lines are the Flory-Huggins calculations using the input parameters provided in Table S2.

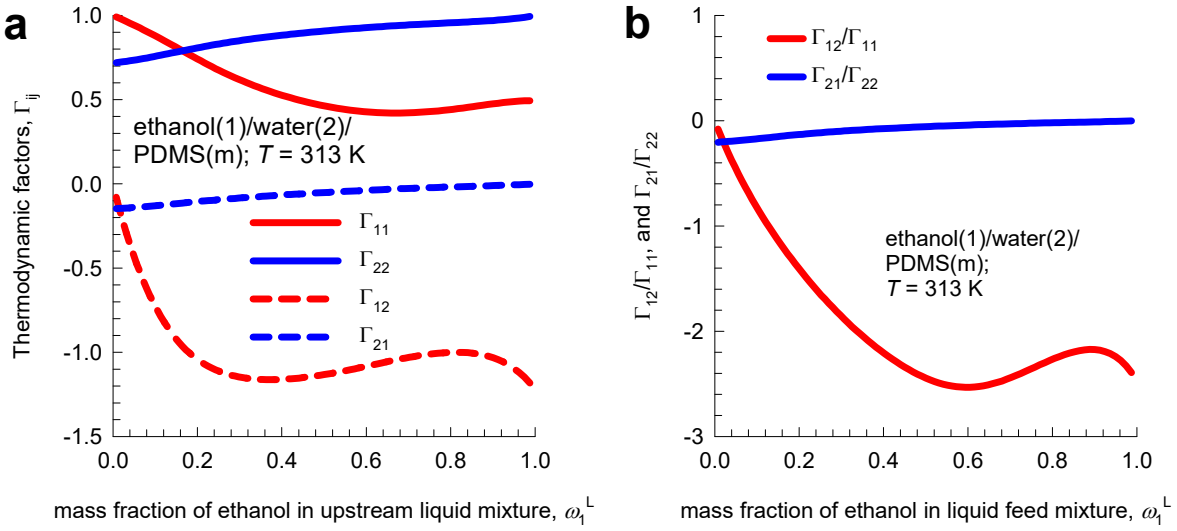

Figure S4. Flory-Huggins calculations of (a) the thermodynamic correction factors, Γ_{ij} and (b) ratios of the elements of thermodynamic correction factors, $\Gamma_{12}/\Gamma_{11}, \Gamma_{21}/\Gamma_{22}$ for sorption equilibrium of ethanol (1) and water (2) in PDMS (m) at 313 K, plotted as function of the mass fraction of ethanol in the liquid feed mixture in the upstream compartment ω_1^L. The F-H parameters are provided in Table S2.

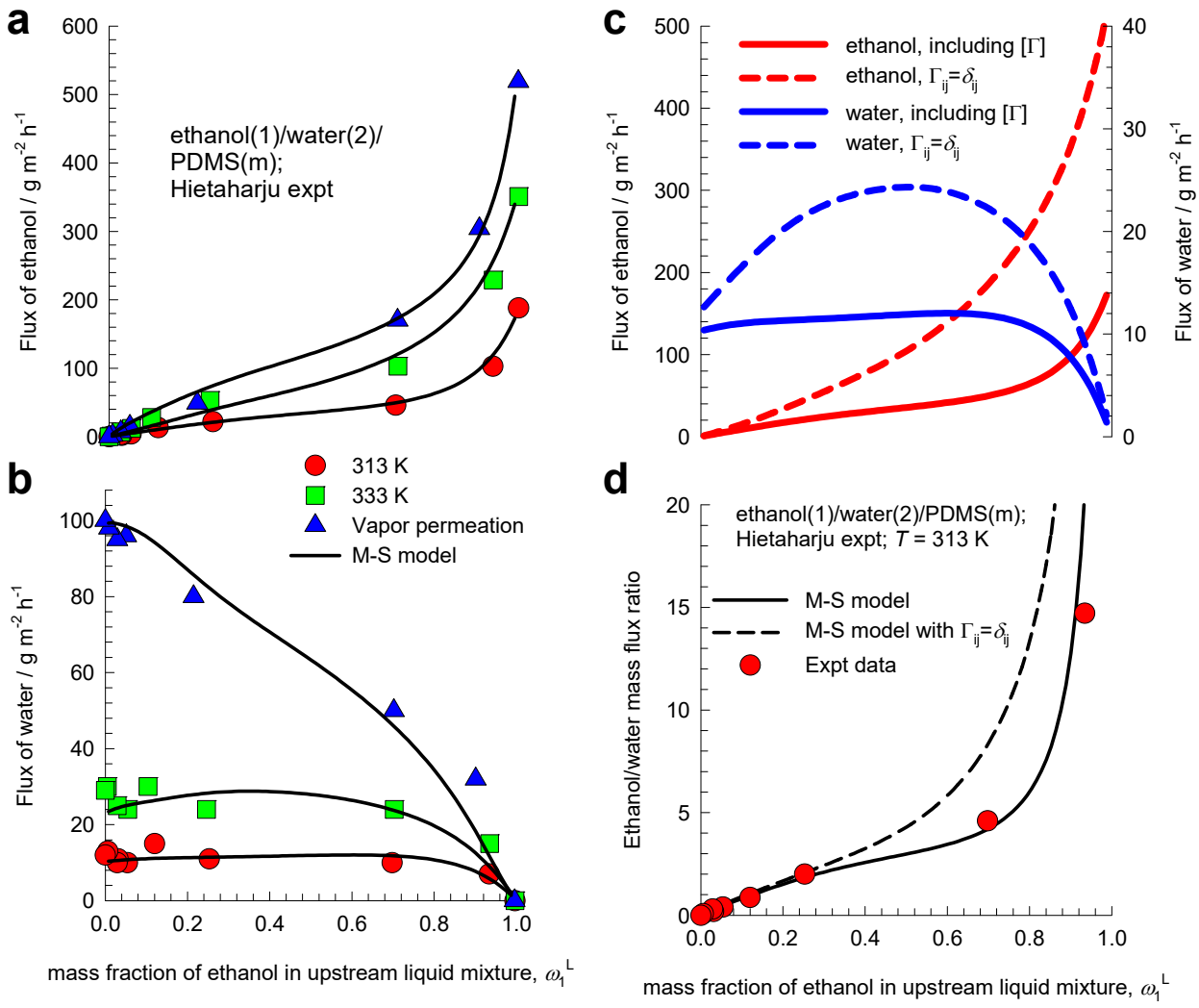

Figure S5. (a, b) Experimental data (indicated by symbols) of Hietaharju et al.[8] for the pervaporation mass fluxes of penetrants ethanol (1) and water (2) across PDMS (m) at 313 K, and 333 K, and vapor permeation, plotted as function of the mass fraction of ethanol in the liquid feed mixture in the upstream compartment ω_1^L. (c) Comparison of the fluxes of ethanol and water at 313 K. (d) Comparison of the ethanol/water mass flux ratios. The continuous solid lines are flux calculations based on eq (S27). The dashed lines are flux calculations in which thermodynamic correction factors are ignored, i.e. $\Gamma_{ij} = \delta_{ij}$. The input diffusivity data are provided in Table S3.

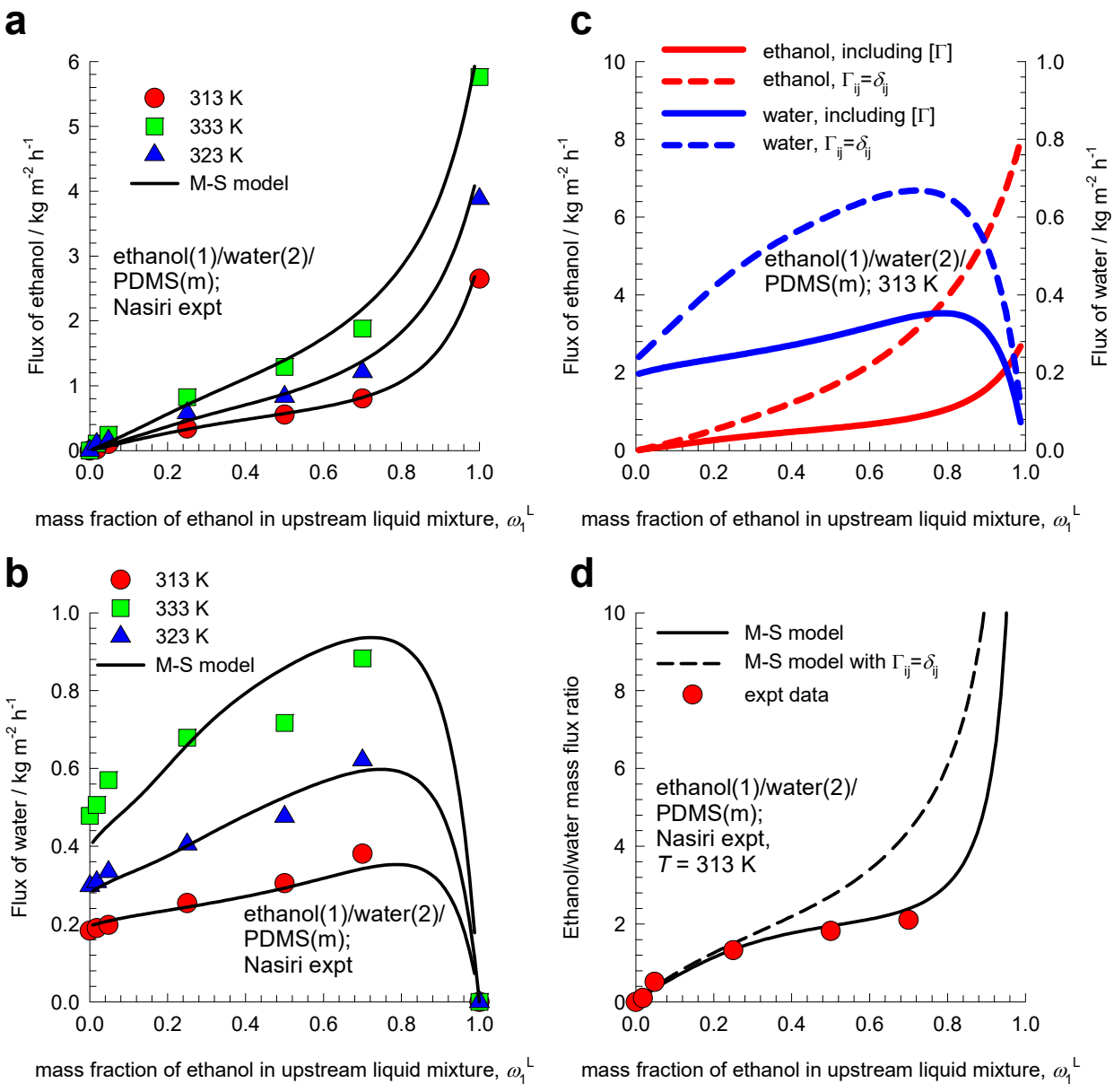

Figure S6. (a, b) Experimental data (indicated by symbols) of Nasiri and Aroujalian,[18] for the mass pervaporation mass fluxes of penetrants ethanol (1) and water (2) across PDMS (m) at 313 K, 323 K, and 333 K, plotted as function of the mass fraction of ethanol in the liquid feed mixture in the upstream compartment ω_1^L. (c) Comparison of the fluxes of ethanol and water at 313 K. . (d) Comparison of the ethanol/water mass flux ratios. The continuous solid lines are flux calculations based on eq (S27). The dashed lines are flux calculations in which thermodynamic correction factors are ignored, i.e. $\Gamma_{ij} = \delta_{ij}$. The input diffusivity data are provided in Table S4.

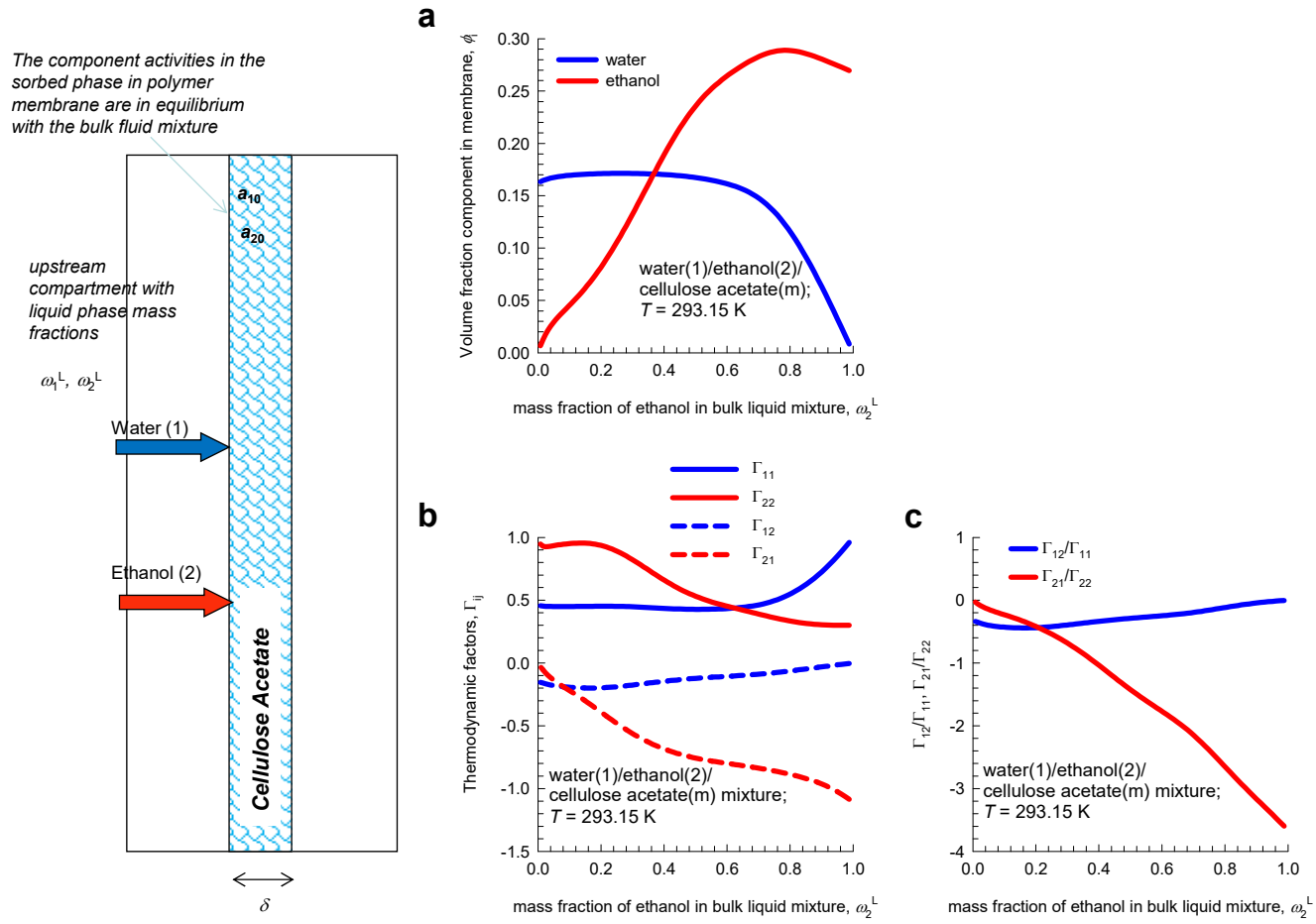

Figure S7. (a) Calculations of the volume fractions of penetrants water (1), ethanol (2) in a cellulose acetate membrane (m) at 293.15 K, plotted as function of the mass fraction of ethanol in the liquid feed mixture in the upstream compartment ω_2^L. (b) Thermodynamic correction factors, Γ_{ij}. (c) Ratios of the elements of thermodynamic correction factors, $\Gamma_{12}/\Gamma_{11}, \Gamma_{21}/\Gamma_{22}$. The Flory-Huggins parameters are specified in Table S5.

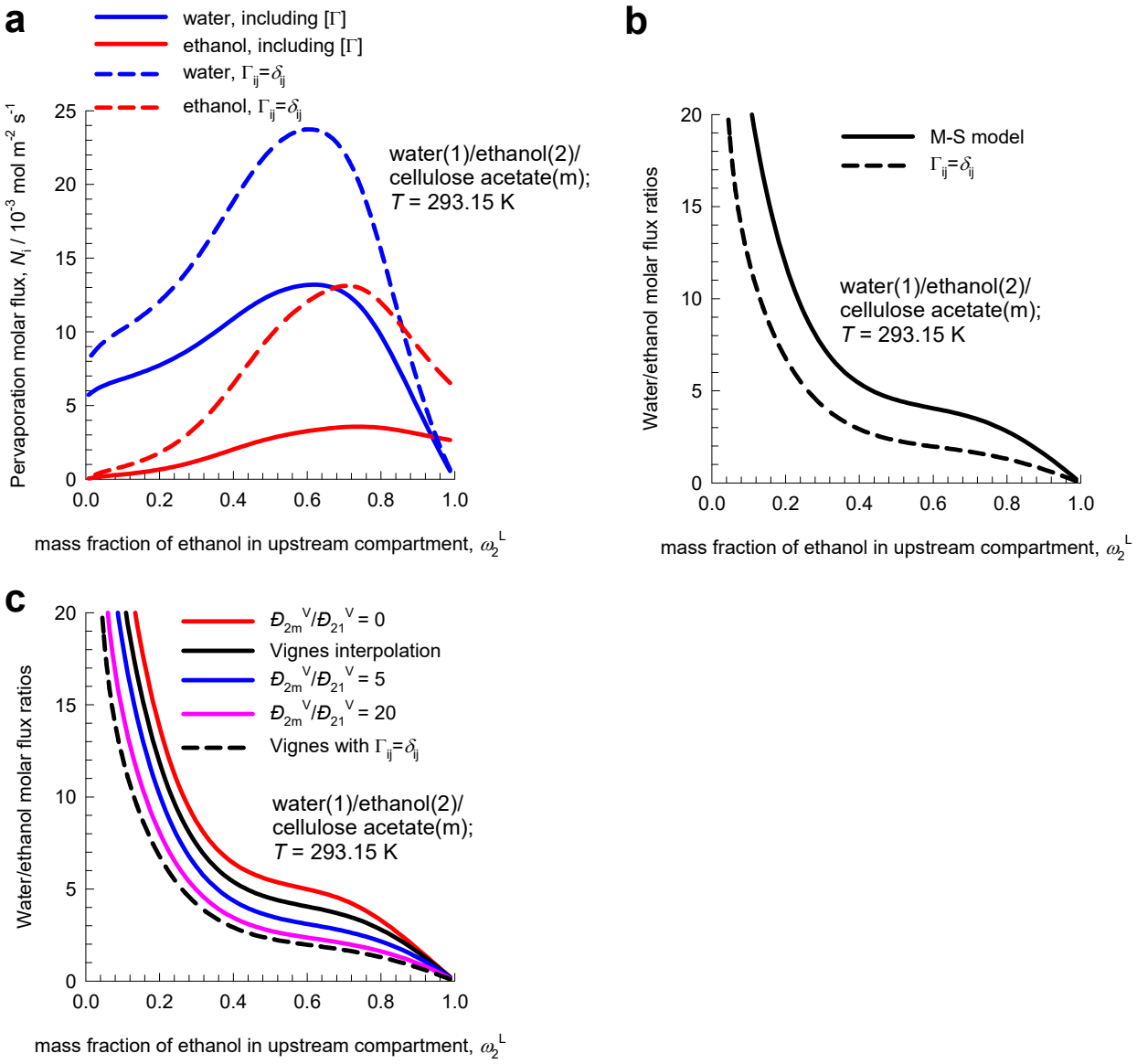

Figure S8. (a) Molar fluxes of water, and ethanol across CA membrane, as function of the mass fraction of ethanol in the liquid feed mixture in the upstream compartment, ω_2^L. (b) Ratio of molar flux of water to that of ethanol, as function of the mass fraction of ethanol in the liquid feed mixture in the upstream compartment, ω_2^L. The continuous solid lines are flux calculations based on eq (S27). The dashed lines are flux calculations in which thermodynamic correction factors are ignored, i.e. $\Gamma_{ij} = \delta_{ij}$. (c) Influence of varying degrees of correlation on the water/ethanol flux ratios. The Flory-Huggins and diffusivity data are specified in Table S5.

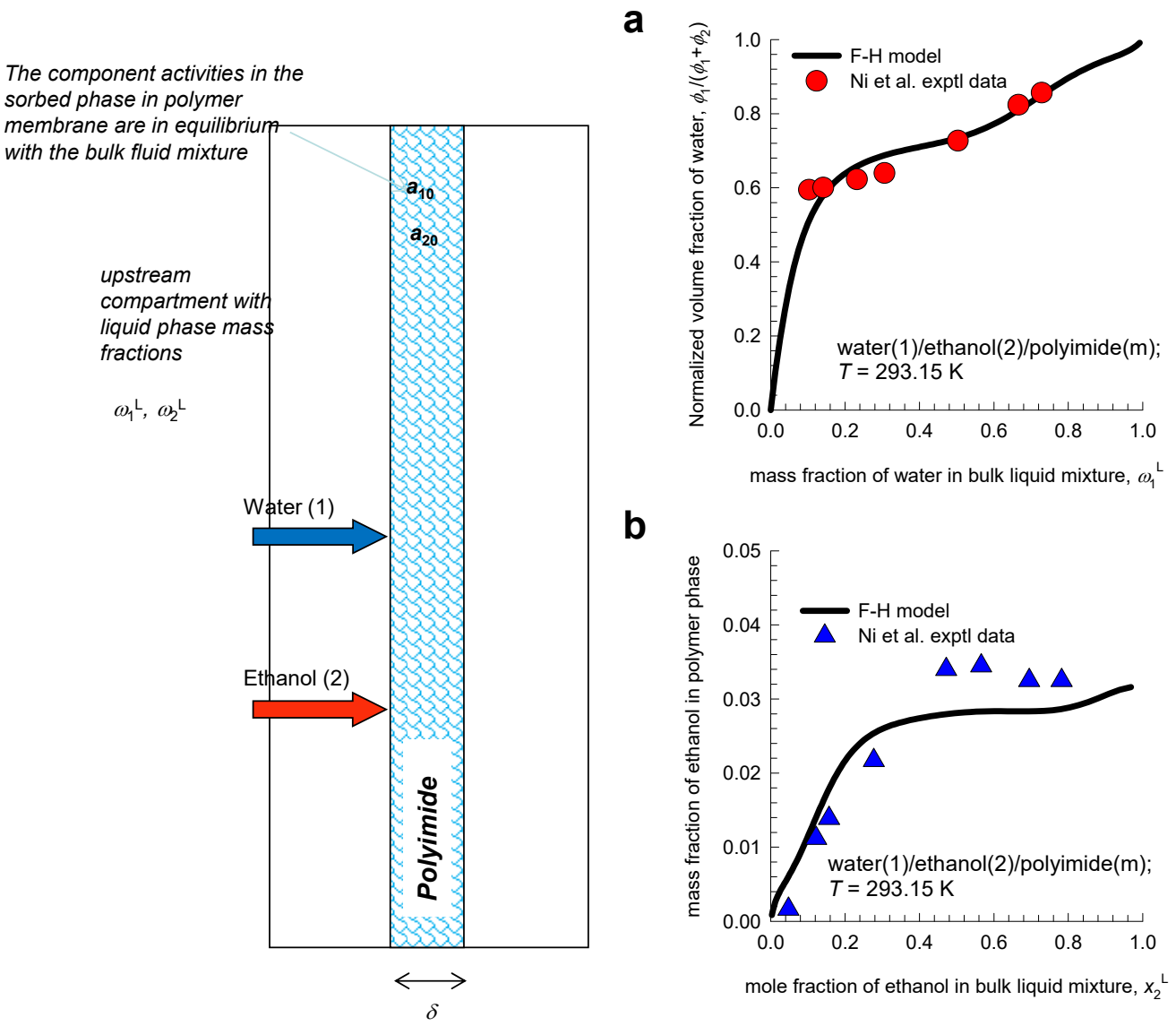

Figure S9. (a, b) Flory-Huggins calculations (continuous solid lines) of the compositions of penetrants (a) water (1), (b) ethanol (2) in polyimide membrane (m) at 293.15 K as a function of the composition of the liquid feed mixture in the upstream compartment. The experimental data (shown by the symbols) are taken from Figure 1 (for ethanol) and Figure 2 (for water) of Ni et al.[23]. The Flory-Huggins parameters are specified in Table S6.

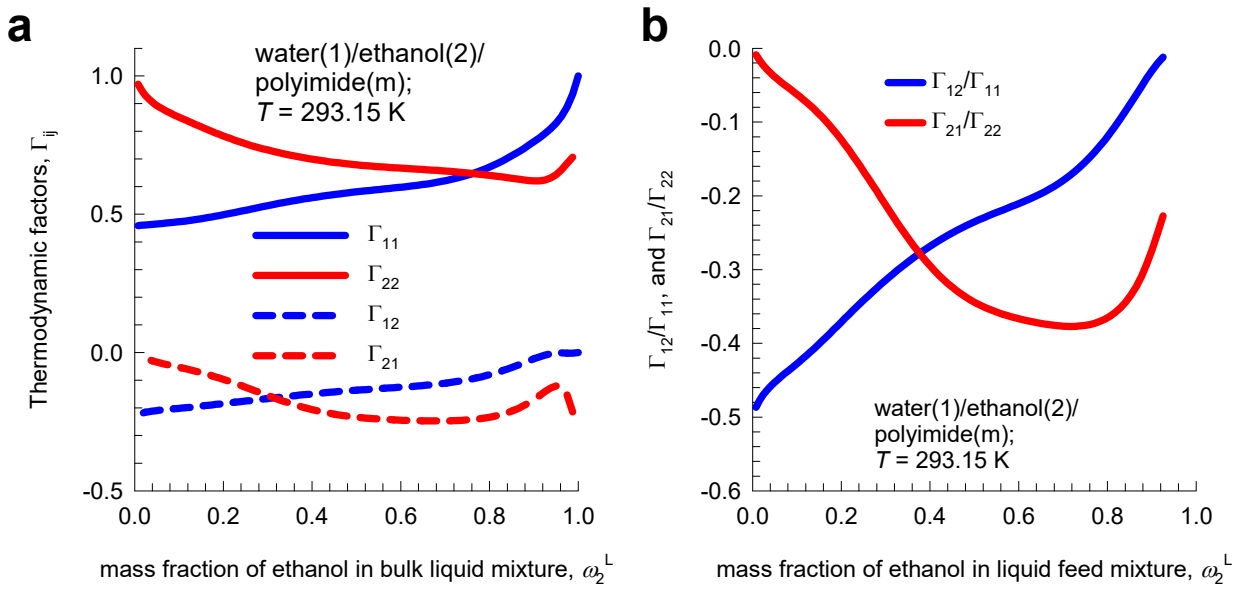

Figure S10. (a) Thermodynamic correction factors factors, Γ_{ij}, for the ternary mixture consisting of water(1), ethanol(2) and polyimide (m), plotted as function of the mass fraction of ethanol (2) in the liquid feed mixture in the upstream compartment ω_2^L. (b) Ratios of the elements of thermodynamic correction factors, $\Gamma_{12}/\Gamma_{11}, \Gamma_{21}/\Gamma_{22}$ as function of the mass fraction of ethanol (2) in the liquid feed mixture in the upstream compartment ω_2^L. The Flory-Huggins parameters are specified in Table S6.

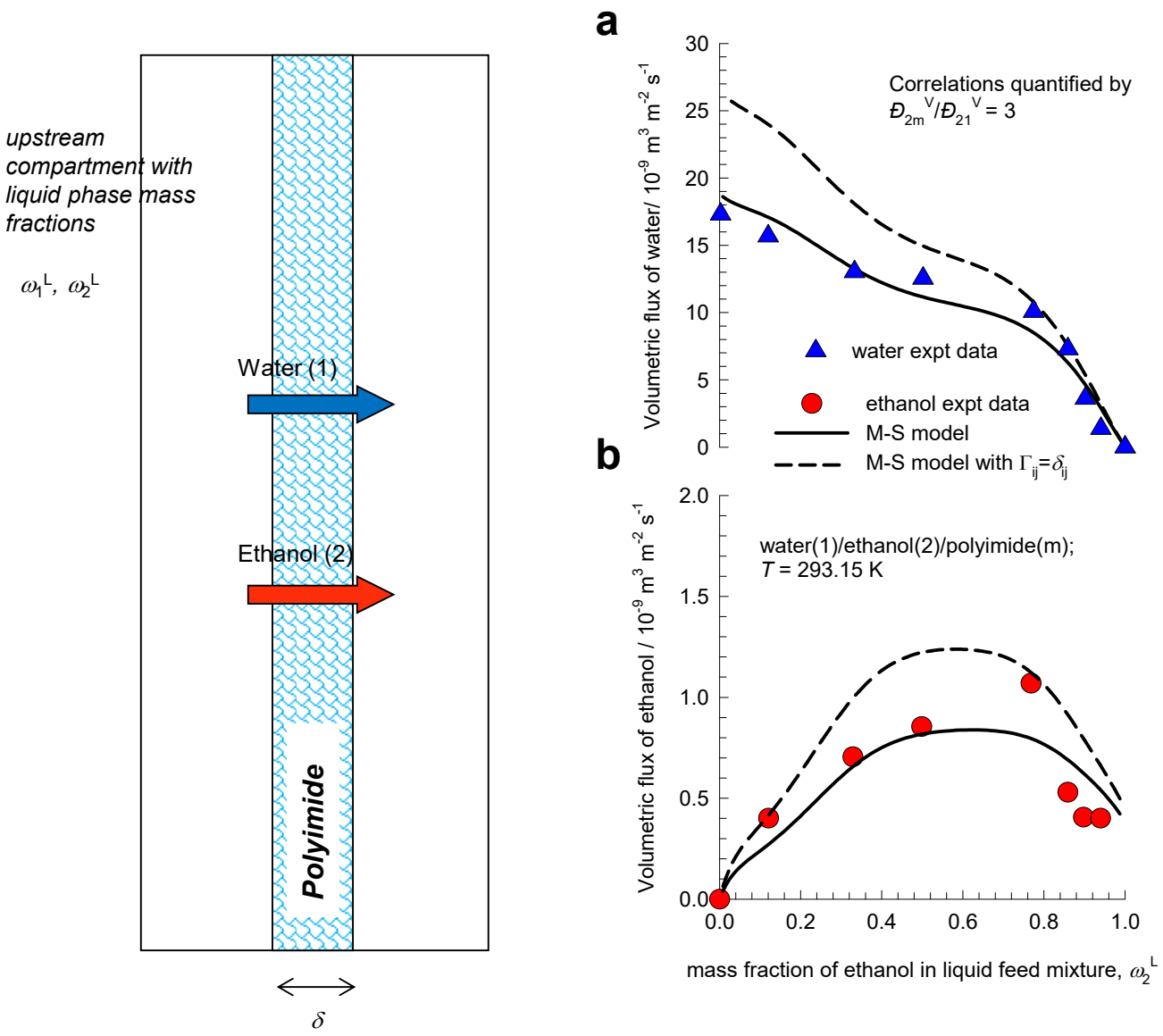

Figure S11. (a, b) Volumetric fluxes of (a) water, and (b) ethanol across polyimide membrane at 293.15 K. The experimental data (shown by the symbols) are taken from Ni et al.[23] The continuous solid lines are flux calculations based on eq (S27); wherein the 1-2 friction is described by $Đ_{2m}^V / Đ_{21}^V = 3$. The dashed lines are flux calculations in which thermodynamic correction factors are ignored, i.e. $\Gamma_{ij} = \delta_{ij}$. The Flory-Huggins and diffusivity data are specified in Table S6.

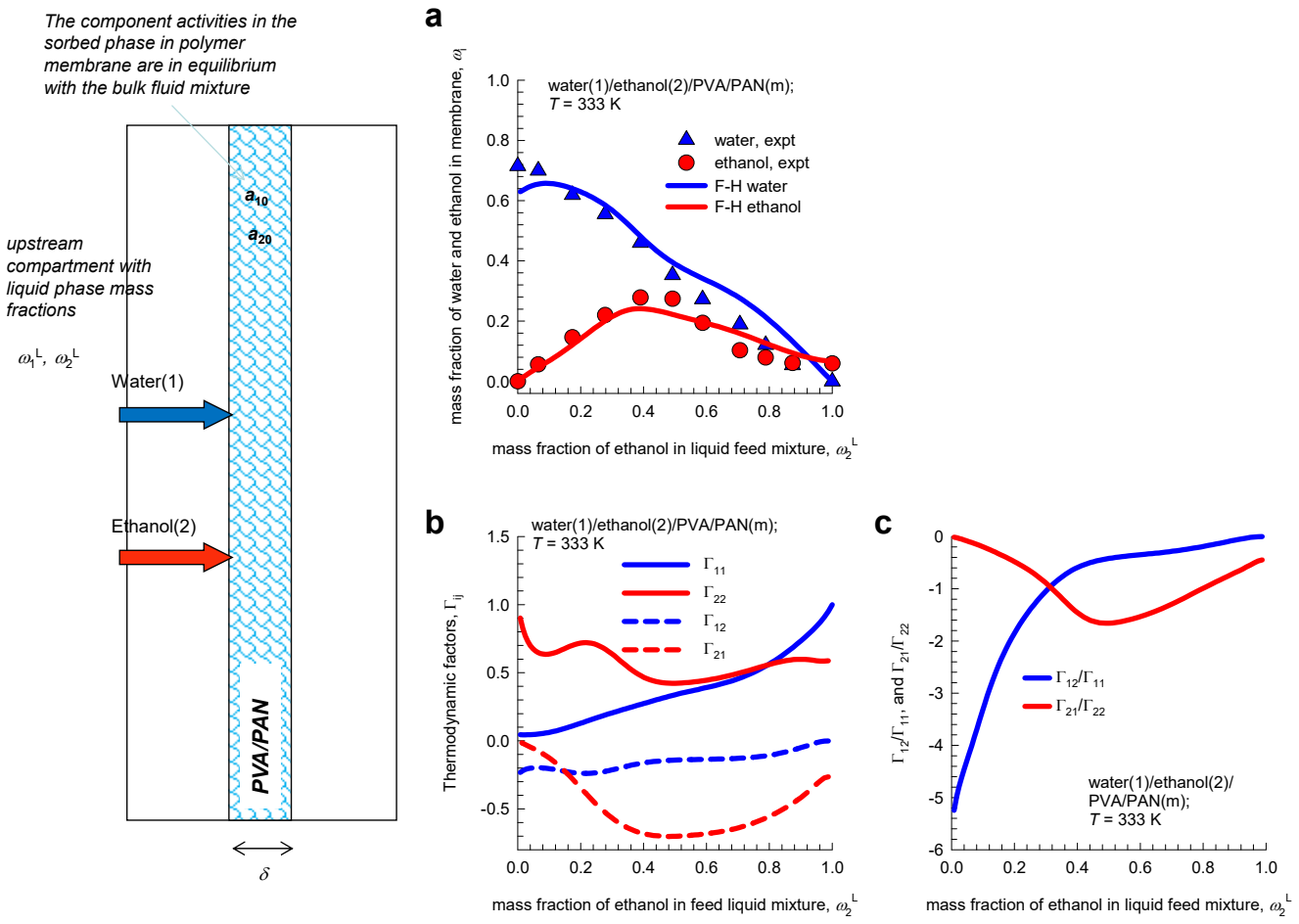

Figure S12. (a) Experimental data (symbols) of Heintz and Stephan[24] for binary sorption of water(1)/ethanol(2) mixtures in poly (vinyl alcohol) /poly (acrylonitrile) (PVA/PAN) composite membrane at 333 K. The *x*-axis is the mass fraction of ethanol(2) in the liquid feed mixture in the upstream compartment ω_2^L. The continuous solid lines are the F-H model calculations using the input data in Table S7. (b) Thermodynamic correction factors factors, Γ_{ij}, plotted as function of the mass fraction of ethanol(2) in the liquid feed mixture in the upstream compartment ω_2^L. (c) Ratios of the elements of thermodynamic correction factors, $\Gamma_{12}/\Gamma_{11}, \Gamma_{21}/\Gamma_{22}$ as function of the mass fraction of ethanol (2) in the liquid feed mixture in the upstream compartment ω_2^L.

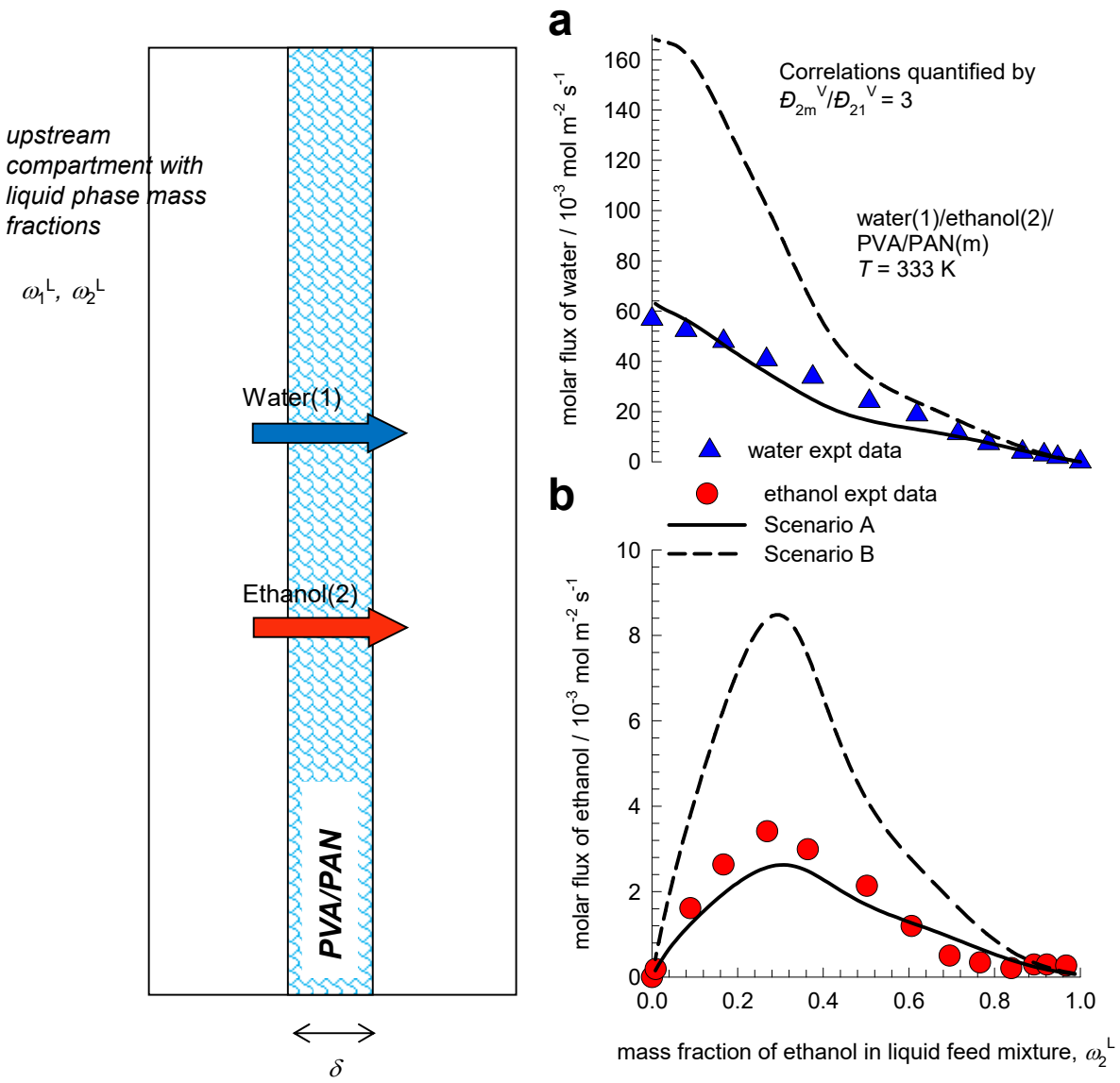

Figure S13. (a, b) Pervaporation fluxes for permeation of water(1)/ethanol(2) mixtures across PVA/PAN composite membrane (m) at 333 K. The experimental data of Heintz and Stephan[25] are indicated by symbols. The continuous solid lines are flux calculations based on eq (S27); wherein the 1-2 friction is described by $Đ_{2m}^V / Đ_{21}^V = 3$. The dashed lines are flux calculations in which thermodynamic correction factors are ignored, i.e. $\Gamma_{ij} = \delta_{ij}$. The Flory-Huggins and diffusivity data are specified in Table S7.

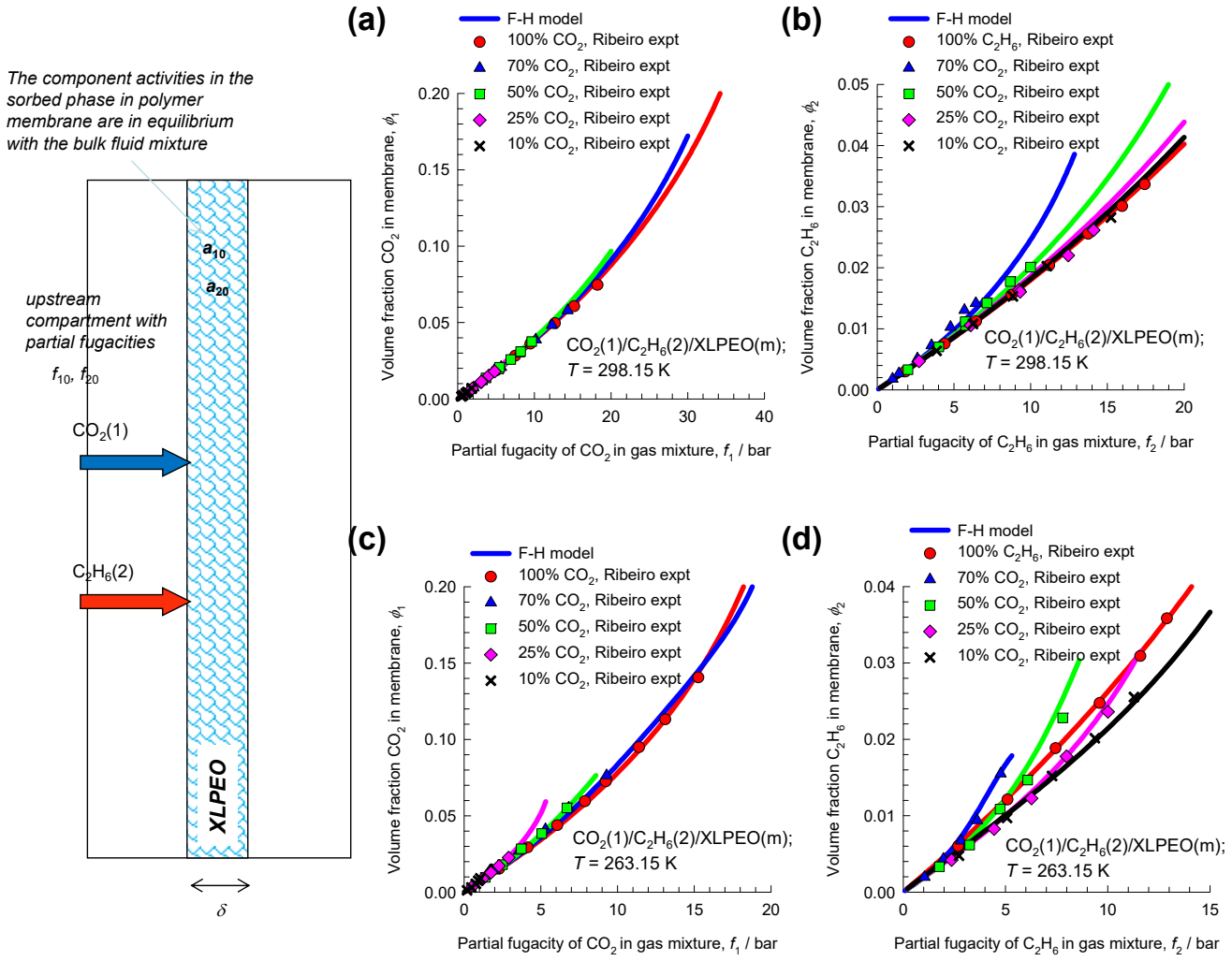

Figure S14. Calculations of the volume fractions of penetrants (a) CO_2 (1) and (b) C_2H_6 (2) in a cross-linked polyethylene oxide (XLPEO) membrane (m) at (a, b) 298.15 K, and (c, d) 263.15. The upstream face of the membrane is in equilibrium with CO_2/C_2H_6 mixtures of five different compositions. The experimental data (symbols) on mixed-gas sorption are those presented in Figures 5 and 6 of Ribeiro and Freeman.[26] The F-H data are summarized in Table S8, and Table S9. In these calculations, the ratio $\frac{\overline{V_1}}{V_m} = 0$, i.e. the molar volume of the penetrant is negligible in comparison to the molar volume of the polymer.

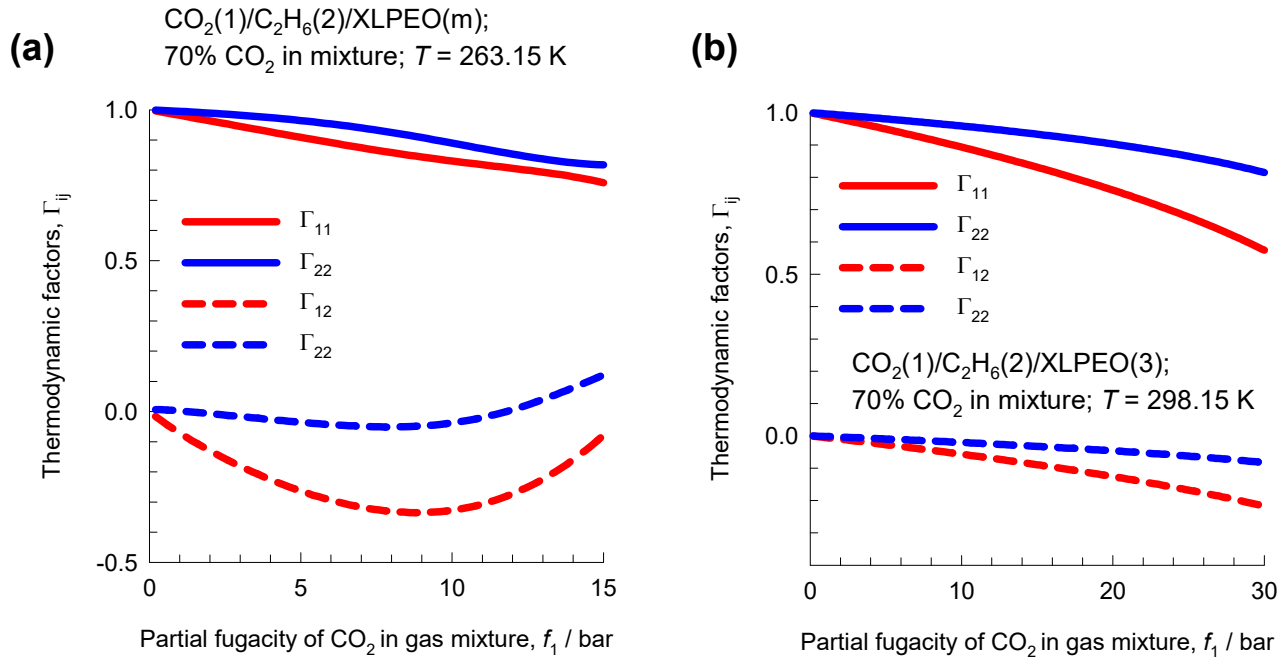

Figure S15. (a, b) Calculations of the elements of the matrix of thermodynamic factors for penetrants CO_2 (component 1) and C_2H_6 (Component 2) in a cross-linked polyethylene oxide (XLPEO) membrane (indicated by subscript m) at (a) 263.15 K, and (b) 298.15 K. The F-H data are summarized in Table S8, and Table S9.

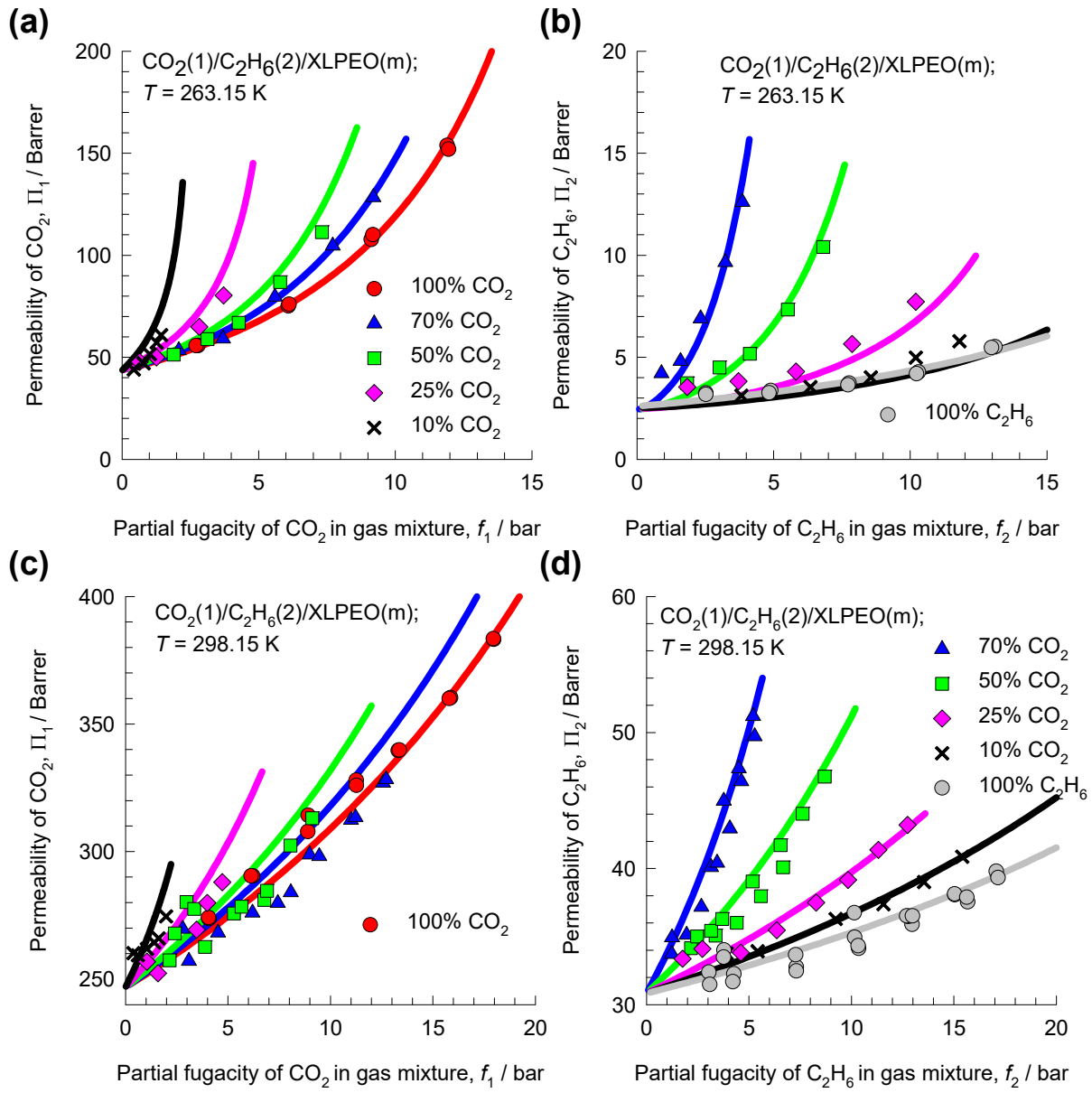

Figure S16. Membrane permeabilities, expressed in Barrers, of (a, c) $CO_2(1)$, and (b, d) $C_2H_6(2)$ for binary $CO_2(1)/C_2H_6(2)$ mixture permeation across a cross-linked polyethylene oxide (XLPEO) membrane at (a, b) 263.15 K, (c, d) 298.15 K. The *x*-axis represents the partial fugacity of (a, c) $CO_2(1)$, and (b, d) $C_2H_6(2)$ in the bulk gas phase in the upstream compartment. The experimental data (symbols) on component permeabilities are those presented in Figures 2, 4, and 5 of Ribeiro et al.[27] The continuous solid lines are the the linearized M-S model predications in which the 1-2 friction is described by $Đ_{2m}^{V} / Đ_{21}^{V} = 4$. The F-H and diffusivity data are summarized in Table S8, and Table S9.

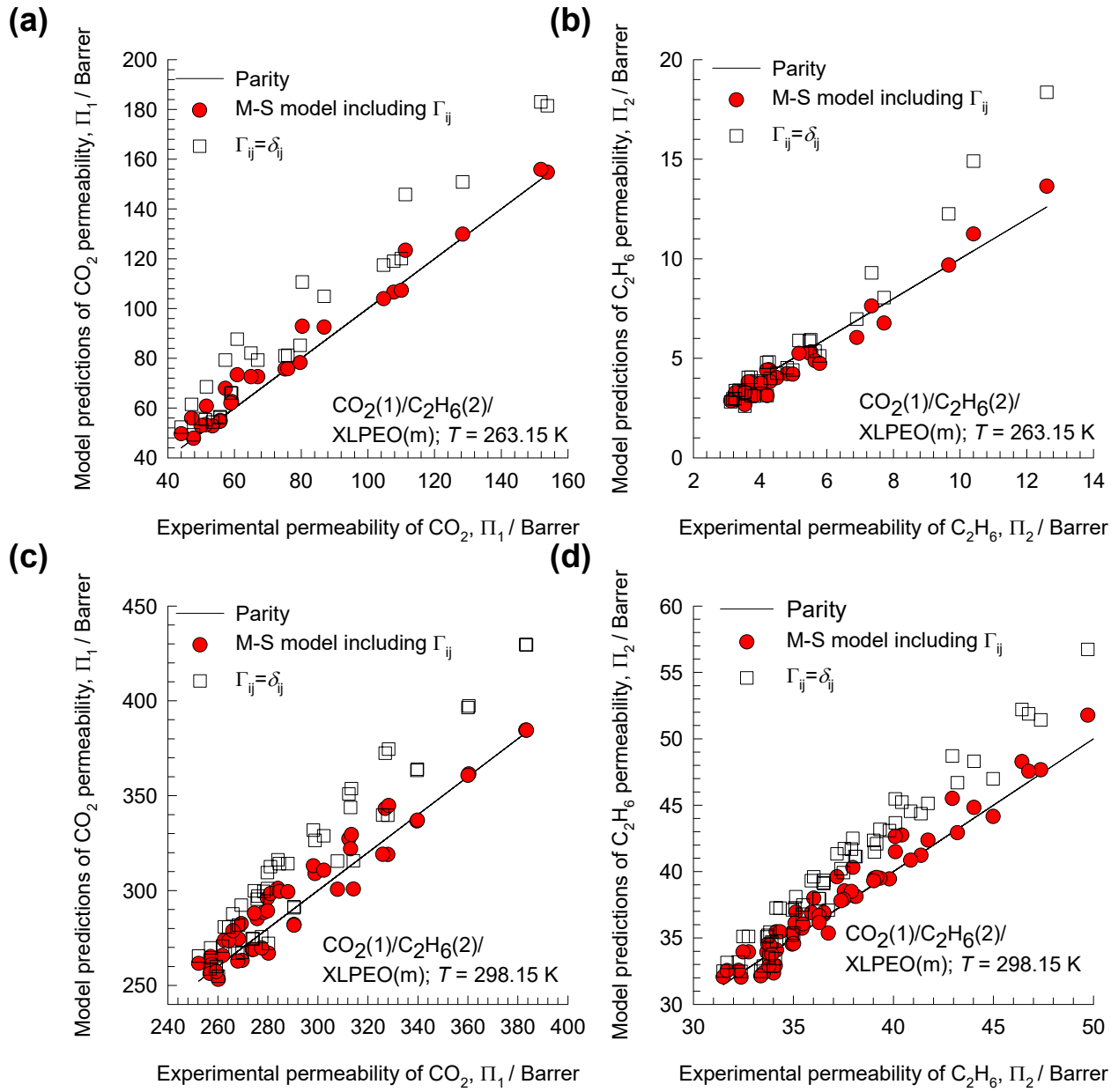

Figure S17. Parity plots comparisons of the experimental data on membrane permeabilities reported by Ribeiro et al.[27] of (a, c) CO_2, and (b, d) C_2H_6 for binary CO_2/C_2H_6 mixture permeation across cross-linked polyethylene oxide (XLPEO) membrane at (a, b) 263.15 K, (c, d) 298.15 K with the model predictions using the linearized M-S model (indicated by red circles) in which the 1-2 friction is described by $Đ_{2m}^{V}/Đ_{21}^{V}=4$. The open squares are the M-S calculations in which the thermodynamic correction factors are ignored, i.e. i.e. $\Gamma_{ij}=\delta_{ij}$. The F-H and diffusivity data are summarized in Table S8, and Table S9.

5 Nomenclature

Latin alphabet

a_i	activity of species *i*, dimensionless
$[B]$	Square matrix containing M-S diffusivities, m^{-2} s
c_i	molar concentration of species *i*, mol m^{-3}
$Đ_{ij}$	M-S diffusivity for binary pair *i-j*, m^2 s^{-1}
$Đ_{ij}^V$	modified M-S diffusivity for binary penetrant pair *i-j*, m^2 s^{-1}
$Đ_{im}^V$	modified M-S diffusivity for penetrant *i* in polymer m, m^2 s^{-1}
f_i	partial fugacity of species *i*, Pa
$f_{i,sat}$	saturation fugacity of species *i*, Pa
$[I]$	Identity matrix with elements δ_{ij}, dimensionless
m	refers to polymer membrane (= species n+1), dimensionless
M_i	molar mass of species *i*, kg mol^{-1}
$\overline{M}$	mean molar mass of mixture, kg mol^{-1}
N_i^{molar}	molar flux of species *i*, mol m^{-2} s^{-1}
N_i^{mass}	molar flux of species *i*, kg m^{-2} s^{-1}
N_i^V	volumetric flux of species *i*, m^3 m^{-2} s^{-1}
n	number of penetrants, dimensionless
p_i	partial pressure of species *i*, Pa
R	gas constant, 8.314 J mol^{-1} K^{-1}
T	absolute temperature, K
$u_2^L = \frac{\phi_2^L}{\phi_1^L + \phi_2^L}$	relative volume fractions in bulk liquid mixture, dimensionless

Nomenclature

$u_2 = \frac{\phi_2}{\phi_1 + \phi_2}$ relative volume fractions in polymer phase, dimensionless

u_i velocity of motion of *i*, m s^{-1}

$\overline{V_i}$ partial molar volume of species *i,* m^3 mol^{-1}

$\overline{V}$ molar volume of mixture*,* m^3 mol^{-1}

z distance coordinate along membrane thickness, m

Greek alphabet

Γ_{ij} thermodynamic factors, dimensionless

$[\Gamma]$ matrix of thermodynamic factors, dimensionless

δ thickness of membrane, m

δ_{ij} Kronecker delta, dimensionless

ε_{ij} plasticization coefficient, dimensionless

$[\Lambda]$ matrix of Maxwell-Stefan diffusivities, m^2 s^{-1}

μ_i molar chemical potential, J mol^{-1}

ϕ_i volume fraction of penetrant *i* in polymer, dimensionless

ϕ_i^L volume fraction in bulk liquid mixture, dimensionless

Π_i permeability of species *i* for polymer membrane, mol m m^{-2} s^{-1} Pa^{-1}

ρ_i mass density of component *i*, kg m^{-3}

χ interaction parameter in Flory-Huggins model, dimensionless

ω_i mass fraction of component *i*, dimensionless

ω_i^L mass fraction of component *i* in liquid phase feed mixture, dimensionless

Subscripts

Nomenclature

i	referring to penetrant *i*
m	referring to membrane
0	upstream face of membrane, $z = 0$
δ	upstream face of membrane, $z = \delta$

Superscripts

V	referring to use of volume fractions

6 References

(1) PTC MathCad 15.0. http://www.ptc.com/, PTC Corporate Headquarters, Needham, 3 November 2015.

(2) Wesselingh, J. A.; Krishna, R. *Mass transfer in multicomponent mixtures*. VSSD: Delft, 2000.

(3) Ribeiro, C. P.; Freeman, B. D. Sorption, Dilation, and Partial Molar Volumes of Carbon Dioxide and Ethane in Cross-Linked Poly(ethylene oxide). *Macromolecules* **2008**, *41*, 9458-9468.

(4) Ribeiro, C. P.; Freeman, B. D. Solubility and Partial Molar Volume of Carbon Dioxide and Ethane in Crosslinked Poly(ethylene oxide) Copolymer. *J. Polym. Sci.: Part B: Polym. Phys.* **2010**, *41*, 9458-9468.

(5) Mulder, M. H. V.; Franken, A. C. M.; Smolders, C. A. Preferential Sorpton versus Preferential Permeability in Pervaporation. *J. Membr. Sci.* **1985**, *22*, 155-178.

(6) Yang, T.-H.; Lue, S. J. Modeling Sorption Behavior for Ethanol/Water Mixtures in a Cross-linked Polydimethylsiloxane Membrane Using the Flory-Huggins Equation. *J. Macromol. Sci., Part B: Phys* **2013**, *52*, 1009-1029.

(7) Varady, M. J.; Pearl, T. P.; Stevenson, S. M.; Mantooth, B. A. Decontamination of VX from Silicone: Characterization of Multicomponent Diffusion Effects. *Ind. Eng. Chem. Res.* **2016**, *55*, 3139-3149.

(8) Hietaharju, J.; Kangas, J.; Tanskanen, J. Analysis of the permeation behavior of ethanol/water mixtures through a polydimethylsiloxane (PDMS) membrane in pervaporation and vapor permeation conditions. *Sep. Purif. Technol.* **2019**, *227*, 115738. https://doi.org/10.1016/j.seppur.2019.115738.

(9) Ribeiro, C. P.; Freeman, B. D.; Paul, D. R. Modeling of Multicomponent Mass Transfer across Polymer Films using a Thermodynamically Consistent Formulation of the Maxwell-Stefan Equations in terms of Volume Fractions. *Polymer* **2011**, *52*, 3970-3983.

(10) Fornasiero, F.; Prausnitz, J. M.; Radke, C. J. Multicomponent Diffusion in Highly Asymmetric Systems. An Extended Maxwell-Stefan Model for Starkly Different-Sized, Segment-Accessible Chain Molecules. *Macromolecules* **2005**, *38*, 1364-1370.

(11) Shao, P.; Huang, R. Y. M. Polymeric membrane pervaporation. *J. Membr. Sci.* **2007**, *287*, 162-179. https://doi.org/10.1016/j.memsci.2006.10.043.

(12) Vignes, A. Diffusion in binary solutions. *Ind. Eng. Chem. Fundamentals* **1966**, *5*, 189-199.

(13) Krishna, R. Describing Mixture Permeation across Polymeric Membranes by a Combination of Maxwell-Stefan and Flory-Huggins Models. *Polymer* **2016**, *103*, 124-131.

(14) Krishna, R. Using the Maxwell-Stefan formulation for Highlighting the Influence of Interspecies (1-2) Friction on Binary Mixture Permeation across Microporous and Polymeric Membranes. *J. Membr. Sci.* **2017**, *540*, 261-276. https://doi.org/10.1016/j.memsci.2017.06.062.

(15) Mulder, M. H. V.; Smolders, C. A. On the Mechanism of Separation of Ethanol/Water Mixtures by Pervaporation. I. Calculation of Concentration Profiles *J. Membr. Sci.* **1984**, *17*, 289-307.

(16) Mulder, M. H. V.; Franken, A. C. M.; Smolders, C. A. On the Mechanism of Separation of Ethanol/Water Mixtures by Pervaporation. II. Experimental Concentration Profiles *J. Membr. Sci.* **1985**, *22*, 41-58.

References

(17) Yang, T.-H.; Lue, S. J. Coupled concentration-dependent diffusivities of ethanol/water mixture sthrough a polymericmembrane:Effect on pervaporative flux and diffusivity profiles. *J. Membr. Sci.* **2013**, *443*, 1-9. https://doi.org/10.1016/j.memsci.2013.05.002.

(18) Nasiri, H.; Aroujalian, A. A Novel Model Based on Cluster Formation for Pervaporation Separation of Polar Components from Aqueous Solutions. *Sep. Purif. Technol.* **2010**, *72*, 13-21.

(19) Favre, E.; Schaetzel, P.; Nguygen, Q. T.; Clément, R.; Néel, J. Sorption, diffusion and vapor permeation of various penetrants through dense poly (dimethylsiloxane) membranes: a transport analysis. *J. Membr. Sci.* **1994**, *92*, 169-184.

(20) Krishna, R.; van Baten, J. M. Hydrogen Bonding Effects in Adsorption of Water-alcohol Mixtures in Zeolites and the Consequences for the Characteristics of the Maxwell-Stefan Diffusivities. *Langmuir* **2010**, *26*, 10854-10867.

(21) Krishna, R.; van Baten, J. M. Highlighting Pitfalls in the Maxwell-Stefan Modeling of Water-Alcohol Mixture Permeation across Pervaporation Membranes. *J. Membr. Sci.* **2010**, *360*, 476-482.

(22) Krishna, R.; van Baten, J. M. Mutual slowing-down effects in mixture diffusion in zeolites. *J. Phys. Chem. C* **2010**, *114*, 13154-13156.

(23) Ni, X.; Sun, X.; Ceng, D. Coupled Diffusion of Water and Ethanol in a Polyimide Membrane. *Polymer Eng. Sci.* **2001**, *41*, 1440-1447.

(24) Heintz, A.; Stephan, W. A generalized solution-diffusion model of the pervaporation process through composite membranes Part I. Prediction of mixture solubilities in the dense active layer using the UNIQUAC model. *J. Membr. Sci.* **1994**, *89*, 143-151.

(25) Heintz, A.; Stephan, W. A generalized solution-diffusion model of the pervaporation process through composite membranes Part II. Concentration polarization, coupled diffusion and the influence of the porous support layer. *J. Membr. Sci.* **1994**, *89*, 153-169.

(26) Ribeiro, C. P.; Freeman, B. D. Carbon Dioxide/ethane Mixed-gas Sorption and Dilation in a Cross-linked Poly(ethylene oxide) Copolymer. *Polymer* **2010**, *51*, 1156-1158.

(27) Ribeiro, C. P.; Freeman, B. D.; Paul, D. R. Pure- and Mixed-Gas Carbon Dioxide/Ethane Permeability and Diffusivity in a Cross-linked Poly(ethylene oxide) Copolymer. *J. Membr. Sci.* **2011**, *377*, 110-123.